Funding: This work was supported by the Else-Kröner-Fresenius-Stiftung (2016_A43 to M.W.), Deutsche Forschungsgemeinschaft (DFG) [SCHN 959/3-1 to G.S.; SFB1321/S01 to M.R., D.S., G.S.; SFB824/C3 to U.K.], Wilhelm-Sander Foundation [2017.048.1 to U.K. and G.S.], Stiftung Charité (to U.K.), Walter-Schulz-Stiftung (to M.W.).

Competing interests

The authors declare that they have no competing interests.

Author contributions

G.S., M.W., C.S. designed the study, analyzed and visualized the data and wrote the paper. K.L., Z.H., S.L., M.J.D., C.S., and R.Ö. performed, interpreted, and analyzed experiments and/or generated important model systems. D.S., R.R., U.K., O.H.K., and M.R. provided important resources and critical input. All authors read and approved the final manuscript.

Abbrevations

4-OHT	4-hydoxytamoxifen
ATF4	activating transcription factor 4
BET	bromodomain and extra terminal motif
CNV	copy number variation
CTD2	cancer target discovery and development network
depmap	dependency map
DoRothEA	discriminant regulon expression analysis
GSEA	gene set enrichment analysis
ICGC	international cancer gene consortium
MYC	myelocytomatosis oncogene
PDAC	pancreatic ductal adenocarcinoma
PERK	proteinkinase RNA-activated-like ER kinase
SUMO	small-ubiquitin-like modifier
TCGA	the cancer genome atlas
UPR	unfolded protein response
UPS	ubiquitin proteasome system

Keywords

MYC, pancreatic cancer, UPR, UPS, proteasome inhibitor, apoptosis

Abstract

Purpose

The myelocytomatosis oncogene (MYC) is an important driver in a subtype of pancreatic ductal adenocarcinoma (PDAC). However, MYC remains a challenging therapeutic target, therefore identifying druggable synthetic lethal interactions in MYC-active PDAC may lead to novel precise therapies.

Methods

Cluster analysis using direct MYC target genes was used to identify PDAC with active MYC. We profiled the transcriptome of established human cell lines, murine primary PDAC cell lines and also accessed public available repositories for transcriptomic profiling. Networks active in MYC hyperactive subtypes were analyzed by gene set enrichment analysis. An unbiased pharmacological drug screen with FDA-approved anti-cancer drugs was conducted to define MYC-associated vulnerabilities, which were validated by analysis of drug response repositories and genetic gain- and loss-of-function experiments.

Results

In an unbiased pharmacological drug screen with FDA-approved anti-cancer drugs we detected that the proteasome inhibitor bortezomib triggers a MYC-associated vulnerability. By integrating publicly available data sets we found the unfolded protein response as a signature connected to MYC. Furthermore, the increased sensitivity of MYC hyperactive PDACs to bortezomib was validated in genetically modified PDAC cells.

Conclusions

In sum, we provide evidence that perturbing the ubiquitin proteasome system might be an option to target MYC hyperactive PDAC cells and our data provide the rationale to further develop precise targeting of the ubiquitin-proteasome system as a subtype-specific therapeutic approach.

Introduction

Pancreatic ductal adenocarcinoma (PDAC) is estimated to become the second leading cause of cancer-related death. In contrast to other solid tumors its prognosis still remains extremely poor [1]. The disease is characterized by a profound intertumoral heterogeneity [2]. Based on various technologies including mRNA sequencing, metabolite profiling, or exon sequencing, distinct molecular subtypes of PDAC associated with different prognosis, biology, and therapeutic responses have been described [2-13]. These data suggest the development of biomarker-driven therapeutic concepts as a promising approach to improve the outcome of the disease. Signatures predicting sensitivity towards the current standard of care chemotherapies are under development [12].

Whole-exome sequencing of micro-dissected PDAC specimen revealed that amplification of MYC (c-MYC) is the only copy number variation (CNV) associated with lower survival rates [14]. These data demonstrate that MYC drives an aggressive subtype of the disease and consistently MYC activity was found to be enriched in the squamous/basal-like/glycolytic subtype [7, 13]. MYC is involved in a variety of biological processes in cancer cells [15]. It is a prominent oncogene acting in concert with mutated *KRAS* in PDAC [16-18]. The transcription factor MYC is an intrinsically disordered protein. Although progress has been made to target MYC [19, 20], it remains a challenge. A strategy to target “undruggables” is to exploit specific cellular dependencies associated with the activity of these proteins [21]**.** Several unbiased genetic screens for synthetic lethal interactions have demonstrated that the MYC protein family confers targetable dependencies [22-26]**,** pointing to a way to define precise therapies. Consistently, MYC has been connected to the increased sensitivity of bromodomain and extra terminal motif (BET) inhibitors [27, 28] and inhibitors of the small-ubiquitin-like modifier (SUMO) pathway in the context of PDAC [29].

To find MYC-associated vulnerabilities, we conducted a limited drug screen and found a connection of MYC to the unfolded protein response (UPR) and an increased sensitivity towards proteasome inhibitors.

Results

Drug screening of FDA-approved anti-cancer drugs identifies vulnerabilities in MYC^{high} human PDAC cells

To identify vulnerabilities in PDACs with an increased MYC activity, we performed an unbiased pharmacological drug screening experiment. To cover the identified MYC^{high} and MYC^{low} subgroups, we used four representative PDAC cell lines with low and high MYC expression (Fig. 1A). Except for PSN1, the doubling time of the cell lines were in similar ranges (Table S1). Gene set enrichment analysis (GSEA) with the GeneTrail2 1.6 web service [30] demonstrated the activation of the MYC network in cells with higher expression of the protein (Fig. 1B). A novel gene set of direct MYC target genes defined by Muhar et al. [31] showed the strongest enrichment in the MYC^{high} cell lines (Fig. 1B). We used the described models for a drug screening experiments with a set of 129 FDA-approved anticancer drugs, which is outlined in figure 2C. Hits were determined as a two-fold difference in the responsiveness of the MYC^{high} models. Among the ten candidates, we identified drugs from different classes, such as HDAC inhibitors, DNA antimetabolites, proteasome inhibitors, topoisomerase inhibitors, and others (Fig. 1D and Table S2).

Validation experiments confirm drug screening results

To validate the single dose drug-screening experiment, we again examined the top 10 hits of our screening experiment using ten different doses and determined the dose-response curves. In addition to the used screening platform, we included a further PDAC line with low MYC protein expression (HPAC) and a PDAC line with intermediate/high MYC expression (MiaPaCa2). As shown in figure 2A, MYC protein expression is significantly different in the analyzed cell lines. Most dose response curves were all left-shifted in the MYC^{high} models (Fig. 2B). Despite the low MYC expression in HPAC cells, these cells cluster into the MYC^{high} high group and show increased sensitivity, which could be explained by expression of functional wild type p53. Although the mean area under the dose response curves (AUC) is lower for all screening hits in the MYC^{high} models, a high variance was detected (Fig. 2B). Such observations point to the need for large cell line panels to ultimate validate screening hits.

HALLMARK- and KEGG-signatures linked to MYC in both datasets. To corroborate the direct connection of such pathways, we used a MYC estrogen receptor fusion protein (MYC^{ER}) of IMIM-PC1 cells, which are characterized by low MYC protein abundance [29]. Here, MYC-

activated signatures show an overlap to the HALLMARK- and KEGG-signatures detected in the analysis of the ICGC and TGCA datasets, pointing to direct effects of MYC (SFig. 1F). Investigating the MYC-connected signatures, we detected a prominent proportion of ribosomal and translational signatures in both datasets, which is well in line with a recent analysis of the TCGA dataset demonstrating that translation is a key process linked to MYC in PDAC [36]. Consistent with increased translational activity, we detected signatures of the unfolded protein response (UPR) and UPR-activated signaling, including Proteinkinase RNA-activated-like ER Kinase (PERK) and Activating Transcription Factor 4 (ATF4) signatures in both investigated human PDAC datasets (Fig. 3E) [37].

MYC and sensitivity towards perturbants of protein homeostasis

The observation that MYC activity is connected to the UPR (Fig. 3D and 3E) and our recent demonstration that MYC is mechanistically involved in the induction of apoptosis in response to proteasome inhibition in PDAC cells [38], prompted us to investigate the bortezomib screening hit in greater detail. First, we used the dependency map (DepMap) portal to access Bortezomib sensitivity data for PDAC cell lines using data from the PRISM repurposing primary screen [39], the GDSC2 screen [40], and the CTD^2 screen [41]. We determined Bortezomib sensitive PDAC cell lines and analyzed them by a gene set enrichment analysis. Consistently, in all three datasets, we observed an enrichment of MYC signatures in the Bortezomib sensitive phenotype (Fig. 4A). To validate a connection of the MYC network to increased sensitivity towards proteasome inhibitors across species, we performed multi-dose drug screenings with the proteasome inhibitors Marizomib and Bortezomib in 38 well-characterized murine *Kras*^{G12D}-driven PDAC cell lines [42] (Fig. 4B). The GI_{50} values of both inhibitors showed a significant correlation (Fig. 4B). We used RNA-seq data [42] of these murine PDAC lines and investigated enrichment of MYC signatures in Bortezomib sensitive, Marizomib sensitive, and lines sensitive to both proteasome inhibitors. We detected enrichment of the MUHAR MYC TARGETS and the HALLMARK MYC TARGETS V2 signature enriched in all proteasome inhibitor sensitive phenotypes (Fig. 4C). To test whether sensitivity of perturbants of the protein homeostasis are commonly connected to increased MYC activity, we analyzed the HSP90

inhibitors Ganetesip and NMS-E973, and the valosin-containing protein (VCP)/p97 inhibitor NMS-873. Such inhibitors are able to induce ER stress and the UPR [43-46]. Two additional proteasome inhibitors, Oprozomib and Ixazomib, were included as controls. To investigate the connection of HSP90 inhibitors and p97 inhibitors to MYC, we used again the data of the PRISM repurposing primary screen [39]. In GSEA, HSP90- and p97-inhibitors sensitive PDAC cell lines enrich for MYC-signatures and an unfolded protein response signature (SFig. 1B). The same was again observed for Oprozomip and Ixazomib sensitive lines (SFig. 1D). These data support the conclusion that MYC hyperactivated PDACs are more sensitive to perturbants of the protein homeostasis.

Human PDAC cells with active MYC are primed for Bortezomib-induced apoptosis

Previously, we described that Bortezomib-induced apoptosis of PDAC cell lines is mediated by MYC-dependent activation of pro-death BCL2 family members, including NOXA (PMAIP1) [38]. To corroborate augmented apoptosis induction as the underlying principle for the increased sensitivity towards proteasome inhibition in MYC^{high} PDAC lines, we monitored cleavage of the caspase substrate PARP over time. Only in MYC^{high} lines, a significant cleavage of PARP was observed eight hours after the treatment (Fig. 4D). 24 hours after the treatment, caspases were also activated in MYC^{low} cell lines (Fig. 4D). Nevertheless, bortezomib induced PARP cleavage was always higher in MYC^{high} lines (Fig. 4E). Since the BH3-only pro-apoptotic BCL2 family member NOXA was recently described to contribute to bortezomib induced apoptosis in PDAC cell lines [38], we induced a CRISPR-Cas9 mediated knockout of the *NOXA* gene in MiaPaCa2 cells (Fig. 4F). The therapeutic response towards Bortezomib is distinctly reduced in *NOXA*-deficient MiaPaCa2 cells (Fig. 4G and 4H), demonstrating the relevance of the gene for the Bortezomib-induced apoptosis.

To analyze the direct contribution of MYC to the proteasome inhibitor sensitivity, we used the dual recombination system [47] with floxed *Myc* alleles [48] to generate a genetic loss of function PDAC model (Fig. 5A). Activation of a Cre^{ERT2} fusion by the addition of 4-hydroxytamoxifen (4-OHT) in this murine PDAC cell lines deleted the floxed *Myc* alleles and reduces MYC protein expression to approximately 30% compared to controls (Fig. 5B and 5C).

It is important to note that we were not able to generate a complete MYC knock-out, due to the profound counter selection of recombination escapers, which underscores the importance of MYC as a target in PDAC. Nevertheless, the MYC-reduced population was less Bortezomib sensitive (Fig. 5D). In addition, we used a conditional gain-of-function model relying on a MYC estrogen receptor fusion (MYC^{ER}). We transduced a murine PDAC cell line with low MYC expression. Upon treatment with 4-hydoxytamoxifen (4-OHT) the MYC targets *Odc1* and *Cad* were induced and endogenous *Myc* was repressed by its negative autoregulation (Fig. 5E). Seeding the cells in 4-OHT for 24 hours followed by a three-day treatment period with Bortezomib, did not change the sensitivity to the proteasome inhibitor (Fig. 5F). MYC-amplified PSN1 cells were included as a Bortezomib sensitive control. Considering the time needed to adapt the system to MYC, we followed two strategies. First, pre-treating the cells with 4-OHT for 24 hours followed by a six-day treatment period with Bortezomib, demonstrated increased sensitivity in the MYC “on” state (Fig. 5G). Second, pretreating the cells with 4-OHT for 96 hours followed by 72 hours of Bortezomib treatment also sensitized the cells to Bortezomib (Fig. 5H). Therefore, gain- and loss-of-function models support the note that MYC modulates the proteasome inhibitor sensitivity of PDAC cells.

are less able to tolerate any further increased protein challenge, contributing to our observation of increased proteasome inhibitor sensitivity in at least some MYC-hyperactive PDACs. Such a scenario is supported by several layers of evidence. It was demonstrated that PDAC cells escaping dependency on KRAS activate the MYC network to increase protein synthesis, which activates adaptive ER-stress pathways [55]. Consistent with our data, such PDAC cells were found to be susceptible to perturbations of protein homeostasis induced by HSP90- or proteasome-inhibitors [55]. Moreover, we found that human PDAC lines sensitive to the Valosin-containing protein (VCP)/p97 inhibitor NMS-873, known to trigger a UPR [45, 46], enrich for MYC signatures. The strong connection of MYC to translation, the observed link to the UPR, the enrichment of MYC signatures in p97 inhibitor or HSP90 inhibitor sensitive PDAC

cell lines, and the modulation of the proteasome inhibitor response in MYC genetic gain- and loss-of-function models [38], argues that MYC hyperactive PDACs are more sensitive towards perturbations of the protein homeostasis. Although these consideration need additional validations in context of PDAC, they are supported from clinical data in multiple myeloma, where MYC seem to be connected to a benefit of proteasome inhibitor based therapy [56, 57]. Some PDAC xenograft *in vivo* models respond to proteasome inhibitor treatment [58, 59], whereas others resist [60]. Also, for patient-derived xenotransplants (PdXs), proteasome inhibitor responding and non-responding models have been documented [61, 62]. Interestingly, Beglyarova et al. observed a proteasome inhibitor response in a MYC-amplified PdX with high protein expression of the oncogene, whereas the non-amplified PdX tested in the study resisted the therapeutic intervention [62]. Such observations clearly demonstrate the need to stratify for responsiveness towards perturbations of protein homeostasis and support our note that proteasome inhibitor sensitivity is a MYC-associated trait in PDAC. The lack of stratification might contribute to the negative outcome of a phase II PDAC study, where patients were treated with Bortezomib or with the combination containing gemcitabine and Bortezomib [63].

In the neuroblastoma line SHEP, which harbors a $MYCN^{ER}$ transgene, an unbiased pharmacological screen with 938 FDA-approved drugs, recently demonstrated Bortezomib, carfilzomib, cabazitaxel, pralatrexate, gemcitabine, vincristine, docetaxel, paclitaxel, etoposide, and doxorubicin to be the top ten MYCN-associated pharmacological vulnerabilities [64]. The substantial overlap of these hits with our screen validates the used experimental approach and demonstrates specific vulnerabilities across the MYC family and cross different tumor entities. As in the PDAC context, where MYC directly activates the transcription of the pro-death BCL2 family member *NOXA* (*PMAIP1*) [38] upon Bortezomib treatment, NOXA contributes also in neuroblastoma models significantly to the Bortezomib-induced apoptosis [64].

The DoRothEA database [32] demonstrates that MYC has the highest number of transcription factor-drug interactions among all transcription factors analyzed [32]. Interestingly, only

associations in which MYC is sensitizing for a drug were observed in this database [32]. Consistently, in context of PDAC, evidence that MYC increases the sensitivity towards proteasome inhibitors, BET inhibitors [27, 28], SUMOylation inhibitors [29], the ERCC3 inhibitor triptolide [62], or Cisplatin [65] was provided. However, it is important to note, that MYC was also associated with drug resistance in PDAC. Important work has demonstrated that MYC is involve in a ductal-neuroendocrine lineage switch, whereby the neuroendocrine lineage resist Gemcitabine [66]. Although paclitaxcel was demonstrated to trigger a mitotic vulnerability [67], recent work, which investigated paclitaxcel-resistant primary PDAC cultures implicates a MYC function in the resistant phenotype [68]. Interestingly, the anti-apoptotic BCL2 family member MCL1 is co-upregulated with MYC in paclitaxel-resistant PDAC cultures [68]. Anti-apoptotic BCL2 family members are described to be relevant modulators of the MYC associated mitotic vulnerability [67]. Whether BCL2 family proteins are important switches, determining MYC mediated sensitivity or resistance in the PDAC context awaits further detailed analysis.

As a mono- as well as in combination-therapies, Bortezomib demonstrates limited efficacy in solid cancers in the clinic [69-71]. Furthermore, a narrow therapeutic index and unfavorable pharmacokinetic features [69, 71], with impaired distribution to solid tumors, may limit the clinical development of Bortezomib in PDAC. However, our data provide evidence that perturbation of the protein homeostasis is an option to target MYC-active PDACs. Considering the development of next-generation proteasome inhibitors [69], the development of new bortezomib formulations [72], or options to target the ubiquitin-proteasome system at different levels [45, 46, 73], will allow to advance the concept in the future.

human PDAC cell lines from the PRISM repurposing primary screen (19Q3) [39], the GDSC2 screen (AUC) [40], and the CTD^2 (AUC) screen [41] were directly accessed and downloaded via the depmap data portal. Bortezomib sensitivity of the lines was divided into quartiles and the most sensitive quartile was investigated for pathway enrichment using gene set enrichment using the complete CCLE-PDAC dataset. For the analysis of drug-MYC interactions we accessed the DoRothEA (Discriminant Regulon Expression Analysis) database [32] (http://dorothea.opentargets.io/) and extracted significant (FDRq < 0.05) drug hits, which are sensitive in cells with an increased MYC expression. Drug hits were summarized in drug classes and compared with hits of our experimental drug screening in a Venn diagram.

PDAC transcriptome data sets of the cancer genome atlas (TCGA) were curated according to Peran et al. [34] (n=150) and mRNA expression data and clinical data were accessed via the GDC data portal (https://portal.gdc.cancer.gov/) [33]. The ICGC dataset was downloaded from the supplemental data of [7]. Acinar cell carcinomas and intraductal papillary mucinous neoplasms were excluded (n=81). TCGA and ICGC datasets were clustered using ClustVis [74] using Euclidean for distance and the Ward method. The datasets were clustered according to the genes of the HALLMARK-MYC-TARGET_V1, HALLMARK-MYC-TARGET_V2, and the direct MYC targets determined by Muhar et al. [31]. PDAC identified by all three signatures were considered as common MYC^{high} PDACs. For the TCGA dataset clustered by HALLMARK-MYC-TARGET_V1, a cluster with incomplete high expression of the target genes was recognized and included in the MYC^{high} group according to this gene set. Survival data was assigned to the commonly MYC^{high} PDAC subtype and displayed in a Kaplan-Meyer-Curve. For subtype association of the common MYC^{high} PDAC, the subtyping of Bailey at al. [7] was used and the Pancreatic progenitor subtype, ADEX subtype, and the Immunogenic subtype were combined and depicted as non-squamous. The TCGA dataset were subtyped according

to ed
IM 3.
En is
(G ith
si m
M es
ar as
do ed
an ng
w

C

C dt,
G /v)
fet in
(Li re
es as
de ng
P M-
P To
sc he
du te
flo for
thi ds
to ne
ce m
W ;

RRID:Addgene_19128) as described [29]. IMIM-PC1MYCER cells were described recently [29].

transfected with a Cas9 expressing px330 vector and the two guides or the pKLV backbone only. Positive transfected MiaPaCa-2 cells were grown under puromycin treatment (1µg/ml) for two weeks. Subsequently single clones were generated, isolated and screened via PCR for knockout clones. The primer-set: C A C T A G T G T G G G C G T A T T A G G (FW) + G A T G T A T T C C A T C T T C C G T T T C C (RV1) reveals a product of 157 bp for knockout cells and 342 bp for wild type cells (data not shown). To further test if both alleles are deleted the primer set: FW + G T T C A G T T T G T C T C C A A A T C T C C (RV2) was used; here a product at 137bp is amplified if the cells harbor a NOXA allele and no product if the cells harbor a knockout for NOXA (Fig. 4C).

Cell lysis and Western blot

To prepare whole-cell extracts RIPA buffer (50 mM Tris, 150 mM NaCl, 1% Nonidet P-40, 0.5% sodium deoxycholate, 0.1% SDS, pH 8.0) supplemented with protease and phosphatase inhibitors (Protease inhibitor cocktail complete EDTA free, Roche Diagnostics, Mannheim, Germany and Phosphatase-Inhibitor-Mix I, Serva, Heidelberg, Germany) was used. Whole-cell extracts were normalized for protein and heated at 95°C for 5 min in protein loading buffer (45.6 mM Tris-HCl pH 6.8, 2% SDS, 10% glycerol, 1% β-mercaptoethanol, 0.01% bromophenol blue) and loaded onto 10-12% SDS-polyacrylamide gels and proteins were transferred to nitrocellulose membranes (Merck-Millipore, Berlin, Germany). Afterwards, membranes were blocked in blocking buffer (5% skim milk, 0.1% Tween in PBS) and incubated with β-Actin (#A5316, Sigma-Aldrich), MYC (#9402, Cell Signaling) and cleaved PARP (552596, BD Pharmingen) primary antibodies. After overnight incubation (4°C) with primary antibodies, membranes were incubated with DyLight™ 680 (#5366S, Cell Signaling) or 800 (#5151S, Cell Signaling) conjugated secondary antibodies (1:10000 dilution). Western blots

were visualized by the Odyssey Infrared Imaging System (Licor, Bad Homburg, Germany) and quantified using the Image Studio Lite Software V 5.2.5 (Licor, Bad Homburg, Germany). Cleaved PARP and MYC expression values were normalized on β-Actin expression and final expression values were calculated out of 3 biological replicates.

Quantitative real time PCR

To isolate RNA from cell lines we followed the manufacturer's instructions of the Maxwell 16 LEV simply RNA Kit (# AS1280) (Promega, Walldorf, Germany). Quantification of mRNA was performed using the BRYT Green® Dye (GoTaq® qPCR, #A600A, Promega) in a real-time PCR analysis system (StepOnePlus, Real-Time PCR System; Applied Biosystems Inc., Carlsbad, CA, USA). Primers used (5'-3'): *Myc*: T T C C T T T G G G C G T T G G A A A C (FW) / G C T G T A C G G A G T C G T A G T C G (RV), *Odc1*: A C A T C C A A A G G C A A A G T T G G (FW) / A G C C T G C T G G T T T T G A G T G T (RV), *Cad*: C T G C C C G G A T T G A T T G A T G T C (FW) / G G T A T T A G G C A T A G C A C A A A C C A (RV) *Gapdh*: G G G T T C C T A T A A A T A C G G A C T G C (FW) / T A C G G C C A A A T C C G T T C A C A (RV). Data analysis was carried out with StepOne software 2.3 Life Technologies/Applied Biosystems/ThermoFisher, Darmstadt, Germany) by the ΔΔCt method (as housekeeping gene *Gapdh* was used) as described [29].

Compounds

The anti-cancer compound library with n=129 drugs was obtained as a plated compound set from the NCI/DTP Open Chemicals Repository (NCI/DTP, MD, USA); the full list of compounds is shown in supplemental table 3. Bortezomib was purchased from LC-Laboratories (Woburn, MA, USA), Marizomib was purchased from Cayman Chemicals (Ann Arbor, MI, USA) and 4-Hydroxytamoxifen (4-OHT) was purchased from Sigma (Sigma, Munich, Germany).

Drug screening experiment

For the drug screen we adapted a recent screening approach [81]. In an attempt to select for drugs highly active in PDAC, we screened PaTu-8988S, Panc1, DanG, and PSN1 cells with a single dose of 600 nM of each drug. Screening was conducted in a 96 well format. 24 hours after the seeding (3.000 cells per well), cells were treated with the drugs of the anti-cancer

compound library for additional 72 hours. Afterwards viability was measured with MTT assays as a read-out for the responsivity. The screen was performed as biological triplicates conducted as technical triplicates. The mean response in the MYC^{high} models was divided by the mean response in the MYC^{low} models. Drugs were ranked according to the ratio and a ratio >2 was defined as a hit.

Viability assay and Clonogenic assay

38 recently characterized [42] murine PDAC cell lines driven by *Kras*$^{G12D/+}$ were termed as PDAC KC cell lines. Cell lines were seeded in a 96 well format. 24 hours after the seeding (1.500 cells per well), cells were treated with the respective drugs for additional 72 hours. Afterwards viability was measured with MTT assays as a read-out for the responsivity. 3-(4,5-Dimethylthiazol-2-yl)-2,5-diphenyltetrazolium bromide (Sigma, Munich, Germany) was used in a dilution of 5 mg/ml. 10 µL of this MTT solution was added per well and incubated for four hours at 37°C. Subsequently the medium was removed and the formazan crystals dissolved in 200 µL DMSO:EtOH (v/v) and incubated for 10 minutes on a horizontal shaker. Absorption was measured at 595 nm on a Thermo/LabSystem Multiskan RC Microplate Reader (Artisan Technology Group, Champaign, IL, USA).

In addition to MTT assay, cellular viability was measured by CellTiter-Glo ATP Viability Assay. Briefly, 25 µl CellTiter-Glo® reagent purchased from Promega (Fitchburg, WI, USA) was added to each well of a 96-well plate 72 hours after drug treatment. After 10 minutes of gentle shaking and 20 minutes of incubation at room temperature, luminescence was measured on a FLUOstar OPTIMA microplate reader (BMG Labtech Ortenberg, Germany). The growth inhibitory 50% (GI_{50}) concentration was calculated with GraphPad Prism 6 (GraphPad Software, CA, USA) using a non-linear regression model. For the clonogenic assay 2.000 MiaPaCa-2 cells (wildtype or NOXA knockout) were seeded in 12-well plates. After 24 hours cells were treated once with the indicated doses of Bortezomib followed by culturing for 14 days in DMEM medium (Life Technologies, Darmstadt, Germany) supplemented with 10% (w/v) fetal calf serum (FCS) (Merck Millipore, Berlin, Germany) and 1% (w/v) penicillin/streptomycin (Life technologies, Darmstadt, Germany). Afterwards the medium was

carefully removed, and cells were washed three times with PBS. The colonies were stained with 0.2% Crystal Violet solution (Sigma by Life Technologies TM, Darmstadt, Germany) for 20 minutes on a shaker at room temperature. To remove background staining, the wells were washed 3 times with tap water, dried and subsequently visualized using a flatbed scanner.

Statistical methods

All experiments were conducted in biological triplicated unless otherwise stated in the figure legends. ANOVA or two-sided Student`s t-test was used to investigate statistical significance, as indicated. p-values were calculated with GraphPad Prism6/8 (GraphPad Software, CA, USA) and corrected according to Bonferroni for multiple testing unless otherwise indicated. p-values are indicated or * in the figures denotes $p < 0.05$. Fisher's exact test, was used to assess the association between PDAC subtypes and the expression of MYC target genes.

Acknowledgment

We thank NCI/DTP Open Chemicals Repository for providing the screening library. The results published here are fully or partially based upon data generated by the Cancer Target Discovery and Development (CTD^2) Network (https://ocg.cancer.gov/programs/ctd2/data-portal) established by the National Cancer Institute's Office of Cancer Genomics. Part of the results shown here are based upon data generated by the TCGA Research Network: https://cancergenome.nih.gov. We thank all colleagues providing plasmids via the Addgene platform. We thank Aylin Aydemir for excellent technical support.

References

1 R.L. Siegel, K.D. Miller and A. Jemal, CA Cancer J Clin 69, 7-34 (2019) doi: 10.3322/caac.21551

2 E.A. Collisson, P. Bailey, D.K. Chang and A.V. Biankin, Nat Rev Gastroenterol Hepatol 16, 207-220 (2019) doi: 10.1038/s41575-019-0109-y

3 a.a.d.h.e. Cancer Genome Atlas Research Network. Electronic address and N. Cancer Genome Atlas Research, Cancer Cell 32, 185-203 e113 (2017) doi: 10.1016/j.ccell.2017.07.007

4 R. Nicolle, Y. Blum, L. Marisa, C. Loncle, O. Gayet, V. Moutardier, O. Turrini, M. Giovannini, B. Bian, M. Bigonnet, M. Rubis, N. Elarouci, L. Armenoult, M. Ayadi, P. Duconseil, M. Gasmi, M. Ouaissi, A. Maignan, G. Lomberk, J.M. Boher, J. Ewald, E. Bories, J. Garnier, A. Goncalves, F. Poizat, J.L. Raoul, V. Secq, S. Garcia, P. Grandval, M. Barraud-Blanc, E. Norguet, M. Gilabert, J.R. Delpero, J. Roques, E. Calvo, F. Guillaumond, S. Vasseur, R. Urrutia, A. de Reynies, N. Dusetti and J. Iovanna, Cell Rep 21, 2458-2470 (2017) doi: 10.1016/j.celrep.2017.11.003

5 E.M. Noll, C. Eisen, A. Stenzinger, E. Espinet, A. Muckenhuber, C. Klein, V. Vogel, B. Klaus, W. Nadler, C. Rosli, C. Lutz, M. Kulke, J. Engelhardt, F.M. Zickgraf, O. Espinosa, M. Schlesner, X. Jiang, A. Kopp-Schneider, P. Neuhaus, M. Bahra, B.V. Sinn, R. Eils, N.A. Giese, T. Hackert, O. Strobel, J. Werner, M.W. Buchler, W. Weichert, A. Trumpp and M.R. Sprick, Nat Med 22, 278-287 (2016) doi: 10.1038/nm.4038

6 N. Waddell, M. Pajic, A.M. Patch, D.K. Chang, K.S. Kassahn, P. Bailey, A.L. Johns, D. Miller, K. Nones, K. Quek, M.C. Quinn, A.J. Robertson, M.Z. Fadlullah, T.J. Bruxner, A.N.

Christ, I. Harliwong, S. Idrisoglu, S. Manning, C. Nourse, E. Nourbakhsh, S. Wani, P.J. Wilson, E. Markham, N. Cloonan, M.J. Anderson, J.L. Fink, O. Holmes, S.H. Kazakoff, C. Leonard, F. Newell, B. Poudel, S. Song, D. Taylor, N. Waddell, S. Wood, Q. Xu, J. Wu, M. Pinese, M.J. Cowley, H.C. Lee, M.D. Jones, A.M. Nagrial, J. Humphris, L.A. Chantrill, V. Chin, A.M. Steinmann, A. Mawson, E.S. Humphrey, E.K. Colvin, A. Chou, C.J. Scarlett, A.V. Pinho, M. Giry-Laterriere, I. Rooman, J.S. Samra, J.G. Kench, J.A. Pettitt, N.D. Merrett, C. Toon, K. Epari, N.Q. Nguyen, A. Barbour, N. Zeps, N.B. Jamieson, J.S. Graham, S.P. Niclou, R. Bjerkvig, R. Grutzmann, D. Aust, R.H. Hruban, A. Maitra, C.A. Iacobuzio-Donahue, C.L. Wolfgang, R.A. Morgan, R.T. Lawlor, V. Corbo, C. Bassi, M. Falconi, G. Zamboni, G. Tortora, M.A. Tempero, I. Australian Pancreatic Cancer Genome, A.J. Gill, J.R. Eshleman, C. Pilarsky, A. Scarpa, E.A. Musgrove, J.V. Pearson, A.V. Biankin and S.M. Grimmond, Nature 518, 495-501 (2015) doi: 10.1038/nature14169

7 P. Bailey, D.K. Chang, K. Nones, A.L. Johns, A.M. Patch, M.C. Gingras, D.K. Miller, A.N. Christ, T.J. Bruxner, M.C. Quinn, C. Nourse, L.C. Murtaugh, I. Harliwong, S. Idrisoglu, S. Manning, E. Nourbakhsh, S. Wani, L. Fink, O. Holmes, V. Chin, M.J. Anderson, S. Kazakoff, C. Leonard, F. Newell, N. Waddell, S. Wood, Q. Xu, P.J. Wilson, N. Cloonan, K.S. Kassahn, D. Taylor, K. Quek, A. Robertson, L. Pantano, L. Mincarelli, L.N. Sanchez, L. Evers, J. Wu, M. Pinese, M.J. Cowley, M.D. Jones, E.K. Colvin, A.M. Nagrial, E.S. Humphrey, L.A. Chantrill, A. Mawson, J. Humphris, A. Chou, M. Pajic, C.J. Scarlett, A.V. Pinho, M. Giry-Laterriere, I. Rooman, J.S. Samra, J.G. Kench, J.A. Lovell, N.D. Merrett, C.W. Toon, K. Epari, N.Q. Nguyen, A. Barbour, N. Zeps, K. Moran-Jones, N.B. Jamieson, J.S. Graham, F. Duthie, K. Oien, J. Hair, R. Grutzmann, A. Maitra, C.A. Iacobuzio-Donahue, C.L. Wolfgang, R.A. Morgan, R.T. Lawlor, V. Corbo, C. Bassi, B. Rusev, P. Capelli, R. Salvia, G. Tortora, D. Mukhopadhyay, G.M. Petersen, I. Australian Pancreatic Cancer Genome, D.M. Munzy, W.E. Fisher, S.A. Karim, J.R. Eshleman, R.H. Hruban, C. Pilarsky, J.P. Morton, O.J. Sansom, A. Scarpa, E.A. Musgrove, U.M. Bailey, O. Hofmann, R.L. Sutherland, D.A. Wheeler, A.J. Gill, R.A. Gibbs, J.V. Pearson,

N. Waddell, A.V. Biankin and S.M. Grimmond, Nature 531, 47-52 (2016) doi: 10.1038/nature16965

8 A. Daemen, D. Peterson, N. Sahu, R. McCord, X. Du, B. Liu, K. Kowanetz, R. Hong, J. Moffat, M. Gao, A. Boudreau, R. Mroue, L. Corson, T. O'Brien, J. Qing, D. Sampath, M. Merchant, R. Yauch, G. Manning, J. Settleman, G. Hatzivassiliou and M. Evangelista, Proc Natl Acad Sci U S A 112, E4410-4417 (2015) doi: 10.1073/pnas.1501605112

9 K.L. Aung, S.E. Fischer, R.E. Denroche, G.H. Jang, A. Dodd, S. Creighton, B. Southwood, S.B. Liang, D. Chadwick, A. Zhang, G.M. O'Kane, H. Albaba, S. Moura, R.C. Grant, J.K. Miller, F. Mbabaali, D. Pasternack, I.M. Lungu, J.M.S. Bartlett, S. Ghai, M. Lemire, S. Holter, A.A. Connor, R.A. Moffitt, J.J. Yeh, L. Timms, P.M. Krzyzanowski, N. Dhani, D. Hedley, F. Notta, J.M. Wilson, M.J. Moore, S. Gallinger and J.J. Knox, Clin Cancer Res 24, 1344-1354 (2018) doi: 10.1158/1078-0432.CCR-17-2994

10 E.A. Collisson, A. Sadanandam, P. Olson, W.J. Gibb, M. Truitt, S. Gu, J. Cooc, J. Weinkle, G.E. Kim, L. Jakkula, H.S. Feiler, A.H. Ko, A.B. Olshen, K.L. Danenberg, M.A. Tempero, P.T. Spellman, D. Hanahan and J.W. Gray, Nat Med 17, 500-503 (2011) doi: 10.1038/nm.2344

11 A. Muckenhuber, A.K. Berger, A.M. Schlitter, K. Steiger, B. Konukiewitz, A. Trumpp, R. Eils, J. Werner, H. Friess, I. Esposito, G. Kloppel, G.O. Ceyhan, M. Jesinghaus, C. Denkert, M. Bahra, A. Stenzinger, M.R. Sprick, D. Jager, C. Springfeld and W. Weichert, Clin Cancer Res 24, 351-359 (2018) doi: 10.1158/1078-0432.CCR-17-2180

12 H. Tiriac, P. Belleau, D.D. Engle, D. Plenker, A. Deschenes, T.D.D. Somerville, F.E.M. Froeling, R.A. Burkhart, R.E. Denroche, G.H. Jang, K. Miyabayashi, C.M. Young, H. Patel, M. Ma, J.F. LaComb, R.L.D. Palmaira, A.A. Javed, J.C. Huynh, M. Johnson, K. Arora, N. Robine, M. Shah, R. Sanghvi, A.B. Goetz, C.Y. Lowder, L. Martello, E. Driehuis, N. LeComte, G. Askan,

C.A. Iacobuzio-Donahue, H. Clevers, L.D. Wood, R.H. Hruban, E. Thompson, A.J. Aguirre, B.M. Wolpin, A. Sasson, J. Kim, M. Wu, J.C. Bucobo, P. Allen, D.V. Sejpal, W. Nealon, J.D. Sullivan, J.M. Winter, P.A. Gimotty, J.L. Grem, D.J. DiMaio, J.M. Buscaglia, P.M. Grandgenett, J.R. Brody, M.A. Hollingsworth, G.M. O'Kane, F. Notta, E. Kim, J.M. Crawford, C. Devoe, A. Ocean, C.L. Wolfgang, K.H. Yu, E. Li, C.R. Vakoc, B. Hubert, S.E. Fischer, J.M. Wilson, R. Moffitt, J. Knox, A. Krasnitz, S. Gallinger and D.A. Tuveson, Cancer Discov 8, 1112-1129 (2018) doi: 10.1158/2159-8290.CD-18-0349

13 J.M. Karasinska, J.T. Topham, S.E. Kalloger, G.H. Jang, R.E. Denroche, L. Culibrk, L.M. Williamson, H.L. Wong, M.K.C. Lee, G.M. O'Kane, R.A. Moore, A.J. Mungall, M.J. Moore, C. Warren, A. Metcalfe, F. Notta, J.J. Knox, S. Gallinger, J. Laskin, M.A. Marra, S.J.M. Jones, D.J. Renouf and D.F. Schaeffer, Clin Cancer Res, (2019) doi: 10.1158/1078-0432.CCR-19-1543

14 A.K. Witkiewicz, E.A. McMillan, U. Balaji, G. Baek, W.C. Lin, J. Mansour, M. Mollaee, K.U. Wagner, P. Koduru, A. Yopp, M.A. Choti, C.J. Yeo, P. McCue, M.A. White and E.S. Knudsen, Nat Commun 6, 6744 (2015) doi: 10.1038/ncomms7744

15 C.V. Dang, Cell 149, 22-35 (2012) doi: 10.1016/j.cell.2012.03.003

16 M. Wirth, S. Mahboobi, O.H. Kramer and G. Schneider, Mol Cancer Ther 15, 1792-1798 (2016) doi: 10.1158/1535-7163.MCT-16-0050

17 M. Wirth and G. Schneider, Trends Cancer 2, 1-3 (2016) doi: 10.1016/j.trecan.2015.12.002

18 E. Hessmann, G. Schneider, V. Ellenrieder and J.T. Siveke, Oncogene 35, 1609-1618 (2016) doi: 10.1038/onc.2015.216

19 B.L. Allen-Petersen and R.C. Sears, BioDrugs 33, 539-553 (2019) doi: 10.1007/s40259-019-00370-5

20 S. Fletcher and E.V. Prochownik, Biochim Biophys Acta 1849, 525-543 (2015) doi: 10.1016/j.bbagrm.2014.03.005

21 A. Huang, L.A. Garraway, A. Ashworth and B. Weber, Nat Rev Drug Discov, (2019) doi: 10.1038/s41573-019-0046-z

22 S. Cermelli, I.S. Jang, B. Bernard and C. Grandori, Cold Spring Harb Perspect Med 4, (2014) doi: 10.1101/cshperspect.a014209

23 S. Herold, J. Kalb, G. Buchel, C.P. Ade, A. Baluapuri, J. Xu, J. Koster, D. Solvie, A. Carstensen, C. Klotz, S. Rodewald, C. Schulein-Volk, M. Dobbelstein, E. Wolf, J. Molenaar, R. Versteeg, S. Walz and M. Eilers, Nature 567, 545-549 (2019) doi: 10.1038/s41586-019-1030-9

24 J.D. Kessler, K.T. Kahle, T. Sun, K.L. Meerbrey, M.R. Schlabach, E.M. Schmitt, S.O. Skinner, Q. Xu, M.Z. Li, Z.C. Hartman, M. Rao, P. Yu, R. Dominguez-Vidana, A.C. Liang, N.L. Solimini, R.J. Bernardi, B. Yu, T. Hsu, I. Golding, J. Luo, C.K. Osborne, C.J. Creighton, S.G. Hilsenbeck, R. Schiff, C.A. Shaw, S.J. Elledge and T.F. Westbrook, Science 335, 348-353 (2012) doi: 10.1126/science.1212728

25 M. Toyoshima, H.L. Howie, M. Imakura, R.M. Walsh, J.E. Annis, A.N. Chang, J. Frazier, B.N. Chau, A. Loboda, P.S. Linsley, M.A. Cleary, J.R. Park and C. Grandori, Proc Natl Acad Sci U S A 109, 9545-9550 (2012) doi: 10.1073/pnas.1121119109

606 26 A.L. Hsieh and C.V. Dang, Recent Results Cancer Res 207, 73-91 (2016) doi:
607 10.1007/978-3-319-42118-6_4
608
609 27 B. Bian, M. Bigonnet, O. Gayet, C. Loncle, A. Maignan, M. Gilabert, V. Moutardier, S.
610 Garcia, O. Turrini, J.R. Delpero, M. Giovannini, P. Grandval, M. Gasmi, M. Ouaissi, V. Secq,
611 F. Poizat, R. Nicolle, Y. Blum, L. Marisa, M. Rubis, J.L. Raoul, J.E. Bradner, J. Qi, G. Lomberk,
612 R. Urrutia, A. Saul, N. Dusetti and J. Iovanna, EMBO Mol Med 9, 482-497 (2017) doi:
613 10.15252/emmm.201606975
614
615 28 B. Bian, N.A. Juiz, O. Gayet, M. Bigonnet, N. Brandone, J. Roques, J. Cros, N. Wang,
616 N. Dusetti and J. Iovanna, Front Oncol 9, 475 (2019) doi: 10.3389/fonc.2019.00475
617
618 29 A. Biederstädt, Z. Hassan, C. Schneeweis, M. Schick, L. Schneider, A. Muckenhuber,
619 Y. Hong, G. Siegers, L. Nilsson, M. Wirth, Z. Dantes, K. Steiger, K. Schunck, S. Langston, H.P.
620 Lenhof, A. Coluccio, F. Orben, J. Slawska, A.K. Scherger, D. Saur, S. Müller, R. Rad, W.
621 Weichert, J. Nilsson, M. Reichert, G. Schneider and U. Keller, Gut, (2020)
622
623 30 D. Stockel, T. Kehl, P. Trampert, L. Schneider, C. Backes, N. Ludwig, A. Gerasch, M.
624 Kaufmann, M. Gessler, N. Graf, E. Meese, A. Keller and H.P. Lenhof, Bioinformatics 32, 1502-
625 1508 (2016) doi: 10.1093/bioinformatics/btv770
626
627 31 M. Muhar, A. Ebert, T. Neumann, C. Umkehrer, J. Jude, C. Wieshofer, P. Rescheneder,
628 J.J. Lipp, V.A. Herzog, B. Reichholf, D.A. Cisneros, T. Hoffmann, M.F. Schlapansky, P. Bhat,
629 A. von Haeseler, T. Kocher, A.C. Obenauf, J. Popow, S.L. Ameres and J. Zuber, Science 360,
630 800-805 (2018) doi: 10.1126/science.aao2793
631

32 L. Garcia-Alonso, F. Iorio, A. Matchan, N. Fonseca, P. Jaaks, G. Peat, M. Pignatelli, F. Falcone, C.H. Benes, I. Dunham, G. Bignell, S.S. McDade, M.J. Garnett and J. Saez-Rodriguez, Cancer Res 78, 769-780 (2018) doi: 10.1158/0008-5472.CAN-17-1679

33 N. Cancer Genome Atlas Research, J.N. Weinstein, E.A. Collisson, G.B. Mills, K.R. Shaw, B.A. Ozenberger, K. Ellrott, I. Shmulevich, C. Sander and J.M. Stuart, Nat Genet 45, 1113-1120 (2013) doi: 10.1038/ng.2764

34 I. Peran, S. Madhavan, S.W. Byers and M.D. McCoy, Clin Cancer Res 24, 3813-3819 (2018) doi: 10.1158/1078-0432.CCR-18-0290

35 M. Chan-Seng-Yue, J.C. Kim, G.W. Wilson, K. Ng, E.F. Figueroa, G.M. O'Kane, A.A. Connor, R.E. Denroche, R.C. Grant, J. McLeod, J.M. Wilson, G.H. Jang, A. Zhang, A. Dodd, S.B. Liang, A. Borgida, D. Chadwick, S. Kalimuthu, I. Lungu, J.M.S. Bartlett, P.M. Krzyzanowski, V. Sandhu, H. Tiriac, F.E.M. Froeling, J.M. Karasinska, J.T. Topham, D.J. Renouf, D.F. Schaeffer, S.J.M. Jones, M.A. Marra, J. Laskin, R. Chetty, L.D. Stein, G. Zogopoulos, B. Haibe-Kains, P.J. Campbell, D.A. Tuveson, J.J. Knox, S.E. Fischer, S. Gallinger and F. Notta, Nat Genet 52, 231-240 (2020) doi: 10.1038/s41588-019-0566-9

36 F.X. Schaub, V. Dhankani, A.C. Berger, M. Trivedi, A.B. Richardson, R. Shaw, W. Zhao, X. Zhang, A. Ventura, Y. Liu, D.E. Ayer, P.J. Hurlin, A.D. Cherniack, R.N. Eisenman, B. Bernard, C. Grandori and N. Cancer Genome Atlas, Cell Syst 6, 282-300 e282 (2018) doi: 10.1016/j.cels.2018.03.003

37 E. Madden, S.E. Logue, S.J. Healy, S. Manie and A. Samali, Biol Cell 111, 1-17 (2019) doi: 10.1111/boc.201800050

38 M. Wirth, N. Stojanovic, J. Christian, M.C. Paul, R.H. Stauber, R.M. Schmid, G. Hacker, O.H. Kramer, D. Saur and G. Schneider, Nucleic Acids Res 42, 10433-10447 (2014) doi: 10.1093/nar/gku763

39 S.M. Corsello, R.T. Nagari, R.D. Spangler, J. Rossen, M. Kocak, J.G. Bryan, R. Humeidi, D. Peck, X. Wu, A.A. Tang, V.M. Wang, S.A. Bender, E. Lemire, R. Narayan, P. Montgomery, U. Ben-David, Y. Chen, M.G. Rees, N.J. Lyons, J.M. McFarland, B.T. Wong, L. Wang, N. Dumont, P.J. O'Hearn, E. Stefan, J.G. Doench, H. Greulich, M. Meyerson, F. Vazquez, A. Subramanian, J.A. Roth, J.A. Bittker, J.S. Boehm, C.C. Mader, A. Tsherniak and T.R. Golub, bioRxiv, 730119 (2019) doi: 10.1101/730119

40 F. Iorio, T.A. Knijnenburg, D.J. Vis, G.R. Bignell, M.P. Menden, M. Schubert, N. Aben, E. Goncalves, S. Barthorpe, H. Lightfoot, T. Cokelaer, P. Greninger, E. van Dyk, H. Chang, H. de Silva, H. Heyn, X. Deng, R.K. Egan, Q. Liu, T. Mironenko, X. Mitropoulos, L. Richardson, J. Wang, T. Zhang, S. Moran, S. Sayols, M. Soleimani, D. Tamborero, N. Lopez-Bigas, P. Ross-Macdonald, M. Esteller, N.S. Gray, D.A. Haber, M.R. Stratton, C.H. Benes, L.F.A. Wessels, J. Saez-Rodriguez, U. McDermott and M.J. Garnett, Cell 166, 740-754 (2016) doi: 10.1016/j.cell.2016.06.017

41 B.A. Aksoy, V. Dancik, K. Smith, J.N. Mazerik, Z. Ji, B. Gross, O. Nikolova, N. Jaber, A. Califano, S.L. Schreiber, D.S. Gerhard, L.C. Hermida, S. Jagu, C. Sander, A. Floratos and P.A. Clemons, Database (Oxford) 2017, (2017) doi: 10.1093/database/bax054

42 S. Mueller, T. Engleitner, R. Maresch, M. Zukowska, S. Lange, T. Kaltenbacher, B. Konukiewitz, R. Ollinger, M. Zwiebel, A. Strong, H.Y. Yen, R. Banerjee, S. Louzada, B. Fu, B. Seidler, J. Gotzfried, K. Schuck, Z. Hassan, A. Arbeiter, N. Schonhuber, S. Klein, C. Veltkamp, M. Friedrich, L. Rad, M. Barenboim, C. Ziegenhain, J. Hess, O.M. Dovey, S. Eser, S. Parekh, F. Constantino-Casas, J. de la Rosa, M.I. Sierra, M. Fraga, J. Mayerle, G. Kloppel, J.

686 Cadinanos, P. Liu, G. Vassiliou, W. Weichert, K. Steiger, W. Enard, R.M. Schmid, F. Yang, K.
687 Unger, G. Schneider, I. Varela, A. Bradley, D. Saur and R. Rad, Nature 554, 62-68 (2018) doi:
688 10.1038/nature25459
689
690 43 E.L. Davenport, H.E. Moore, A.S. Dunlop, S.Y. Sharp, P. Workman, G.J. Morgan and
691 F.E. Davies, Blood 110, 2641-2649 (2007) doi: 10.1182/blood-2006-11-053728
692
693 44 C. Gallerne, A. Prola and C. Lemaire, Biochim Biophys Acta 1833, 1356-1366 (2013)
694 doi: 10.1016/j.bbamcr.2013.02.014
695
696 45 P.H. Vekaria, T. Home, S. Weir, F.J. Schoenen and R. Rao, Front Oncol 6, 181 (2016)
697 doi: 10.3389/fonc.2016.00181
698
699 46 P. Magnaghi, R. D'Alessio, B. Valsasina, N. Avanzi, S. Rizzi, D. Asa, F. Gasparri, L.
700 Cozzi, U. Cucchi, C. Orrenius, P. Polucci, D. Ballinari, C. Perrera, A. Leone, G. Cervi, E.
701 Casale, Y. Xiao, C. Wong, D.J. Anderson, A. Galvani, D. Donati, T. O'Brien, P.K. Jackson and
702 A. Isacchi, Nat Chem Biol 9, 548-556 (2013) doi: 10.1038/nchembio.1313
703
704 47 N. Schonhuber, B. Seidler, K. Schuck, C. Veltkamp, C. Schachtler, M. Zukowska, S.
705 Eser, T.B. Feyerabend, M.C. Paul, P. Eser, S. Klein, A.M. Lowy, R. Banerjee, F. Yang, C.L.
706 Lee, E.J. Moding, D.G. Kirsch, A. Scheideler, D.R. Alessi, I. Varela, A. Bradley, A. Kind, A.E.
707 Schnieke, H.R. Rodewald, R. Rad, R.M. Schmid, G. Schneider and D. Saur, Nat Med 20, 1340-
708 1347 (2014) doi: 10.1038/nm.3646
709
710 48 I.M. de Alboran, R.C. O'Hagan, F. Gartner, B. Malynn, L. Davidson, R. Rickert, K.
711 Rajewsky, R.A. DePinho and F.W. Alt, Immunity 14, 45-55 (2001) doi: 10.1016/s1074-
712 7613(01)00088-7

713 49 A.J. Wolpaw and C.V. Dang, Biochim Biophys Acta Rev Cancer 1870, 43-50 (2018)
714 doi: 10.1016/j.bbcan.2018.05.003
715
716 50 M. Barna, A. Pusic, O. Zollo, M. Costa, N. Kondrashov, E. Rego, P.H. Rao and D.
717 Ruggero, Nature 456, 971-975 (2008) doi: 10.1038/nature07449
718
719 51 L.S. Hart, J.T. Cunningham, T. Datta, S. Dey, F. Tameire, S.L. Lehman, B. Qiu, H.
720 Zhang, G. Cerniglia, M. Bi, Y. Li, Y. Gao, H. Liu, C. Li, A. Maity, A. Thomas-Tikhonenko, A.E.
721 Perl, A. Koong, S.Y. Fuchs, J.A. Diehl, I.G. Mills, D. Ruggero and C. Koumenis, J Clin Invest
722 122, 4621-4634 (2012) doi: 10.1172/JCI62973
723
724 52 P. Nagy, A. Varga, K. Pircs, K. Hegedus and G. Juhasz, PLoS Genet 9, e1003664
725 (2013) doi: 10.1371/journal.pgen.1003664
726
727 53 N. Zhao, J. Cao, L. Xu, Q. Tang, L.E. Dobrolecki, X. Lv, M. Talukdar, Y. Lu, X. Wang,
728 D.Z. Hu, Q. Shi, Y. Xiang, Y. Wang, X. Liu, W. Bu, Y. Jiang, M. Li, Y. Gong, Z. Sun, H. Ying,
729 B. Yuan, X. Lin, X.H. Feng, S.M. Hartig, F. Li, H. Shen, Y. Chen, L. Han, Q. Zeng, J.B.
730 Patterson, B.A. Kaipparettu, N. Putluri, F. Sicheri, J.M. Rosen, M.T. Lewis and X. Chen, J Clin
731 Invest 128, 1283-1299 (2018) doi: 10.1172/JCI95873
732
733 54 H. Xie, C.H. Tang, J.H. Song, A. Mancuso, J.R. Del Valle, J. Cao, Y. Xiang, C.V. Dang,
734 R. Lan, D.J. Sanchez, B. Keith, C.C. Hu and M.C. Simon, J Clin Invest 128, 1300-1316 (2018)
735 doi: 10.1172/JCI95864
736
737 55 G. Genovese, A. Carugo, J. Tepper, F.S. Robinson, L. Li, M. Svelto, L. Nezi, D. Corti,
738 R. Minelli, P. Pettazzoni, T. Gutschner, C.C. Wu, S. Seth, K.C. Akdemir, E. Leo, S. Amin, M.D.
739 Molin, H. Ying, L.N. Kwong, S. Colla, K. Takahashi, P. Ghosh, V. Giuliani, F. Muller, P. Dey,
740 S. Jiang, J. Garvey, C.G. Liu, J. Zhang, T.P. Heffernan, C. Toniatti, J.B. Fleming, M.G.

741 Goggins, L.D. Wood, A. Sgambato, A. Agaimy, A. Maitra, C.W. Roberts, H. Wang, A. Viale,
742 R.A. DePinho, G.F. Draetta and L. Chin, Nature 542, 362-366 (2017) doi:
743 10.1038/nature21064
744
745 56 W.J. Chng, G.F. Huang, T.H. Chung, S.B. Ng, N. Gonzalez-Paz, T. Troska-Price, G.
746 Mulligan, M. Chesi, P.L. Bergsagel and R. Fonseca, Leukemia 25, 1026-1035 (2011) doi:
747 10.1038/leu.2011.53
748
749 57 A. Di Bacco, N.J. Bahlis, N.C. Munshi, H. Avet-Loiseau, T. Masszi, L. Viterbo, L. Pour,
750 P. Ganly, M. Cavo, C. Langer, S.K. Kumar, S.V. Rajkumar, J.J. Keats, D. Berg, J. Lin, B. Li, S.
751 Badola, L. Shen, J. Zhang, D.L. Esseltine, K. Luptakova, H. van de Velde, P.G. Richardson
752 and P. Moreau, Eur J Haematol, (2020) doi: 10.1111/ejh.13405
753
754 58 S.T. Nawrocki, B. Sweeney-Gotsch, R. Takamori and D.J. McConkey, Mol Cancer Ther
755 3, 59-70 (2004)
756
757 59 C.M. Sloss, F. Wang, R. Liu, L. Xia, M. Houston, D. Ljungman, M.A. Palladino and J.C.
758 Cusack, Jr., Clin Cancer Res 14, 5116-5123 (2008) doi: 10.1158/1078-0432.CCR-07-4506
759
760 60 A. Marten, N. Zeiss, S. Serba, S. Mehrle, M. von Lilienfeld-Toal and J. Schmidt, Mol
761 Cancer Ther 7, 3624-3631 (2008) doi: 10.1158/1535-7163.MCT-08-0393
762
763 61 K. Kawaguchi, K. Igarashi, T. Murakami, T. Kiyuna, T.M. Lwin, H.K. Hwang, J.C.
764 Delong, B.M. Clary, M. Bouvet, M. Unno and R.M. Hoffman, Oncotarget 8, 47490-47496 (2017)
765 doi: 10.18632/oncotarget.17667
766
767 62 N. Beglyarova, E. Banina, Y. Zhou, R. Mukhamadeeva, G. Andrianov, E. Bobrov, E.
768 Lysenko, N. Skobeleva, L. Gabitova, D. Restifo, M. Pressman, I.G. Serebriiskii, J.P. Hoffman,

769 K. Paz, D. Behrens, V. Khazak, S.A. Jablonski, E.A. Golemis, L.M. Weiner and I. Astsaturov,
770 Clin Cancer Res 22, 6153-6163 (2016) doi: 10.1158/1078-0432.CCR-16-0149
771
772 63 S.R. Alberts, N.R. Foster, R.F. Morton, J. Kugler, P. Schaefer, M. Wiesenfeld, T.R.
773 Fitch, P. Steen, G.P. Kim and S. Gill, Ann Oncol 16, 1654-1661 (2005) doi:
774 10.1093/annonc/mdi324
775
776 64 J. Wang, J. Jiang, H. Chen, L. Wang, H. Guo, L. Yang, D. Xiao, G. Qing and H. Liu,
777 Oncogene 38, 6737-6751 (2019) doi: 10.1038/s41388-019-0912-5
778
779 65 H. Biliran, Jr., S. Banerjee, A. Thakur, F.H. Sarkar, A. Bollig, F. Ahmed, J. Wu, Y. Sun
780 and J.D. Liao, Clin Cancer Res 13, 2811-2821 (2007) doi: 10.1158/1078-0432.CCR-06-1844
781
782 66 A.S. Farrell, M.M. Joly, B.L. Allen-Petersen, P.J. Worth, C. Lanciault, D. Sauer, J. Link,
783 C. Pelz, L.M. Heiser, J.P. Morton, N. Muthalagu, M.T. Hoffman, S.L. Manning, E.D. Pratt, N.D.
784 Kendsersky, N. Egbukichi, T.S. Amery, M.C. Thoma, Z.P. Jenny, A.D. Rhim, D.J. Murphy, O.J.
785 Sansom, H.C. Crawford, B.C. Sheppard and R.C. Sears, Nat Commun 8, 1728 (2017) doi:
786 10.1038/s41467-017-01967-6
787
788 67 C. Topham, A. Tighe, P. Ly, A. Bennett, O. Sloss, L. Nelson, R.A. Ridgway, D. Huels,
789 S. Littler, C. Schandl, Y. Sun, B. Bechi, D.J. Procter, O.J. Sansom, D.W. Cleveland and S.S.
790 Taylor, Cancer Cell 28, 129-140 (2015) doi: 10.1016/j.ccell.2015.06.001
791
792 68 E. Parasido, G.S. Avetian, A. Naeem, G. Graham, M. Pishvaian, E. Glasgow, S.
793 Mudambi, Y. Lee, C. Ihemelandu, M. Choudhry, I. Peran, P.P. Banerjee, M.L. Avantaggiati, K.
794 Bryant, E. Baldelli, M. Pierobon, L. Liotta, E. Petricoin, S.T. Fricke, A. Sebastian, J. Cozzitorto,
795 G.G. Loots, D. Kumar, S. Byers, E. Londin, A. DiFeo, G. Narla, J. Winter, J.R. Brody, O.

796 Rodriguez and C. Albanese, Mol Cancer Res 17, 1815-1827 (2019) doi: 10.1158/1541-
797 7786.MCR-19-0191
798
799 69 E.E. Manasanch and R.Z. Orlowski, Nat Rev Clin Oncol 14, 417-433 (2017) doi:
800 10.1038/nrclinonc.2016.206
801
802 70 Z. Huang, Y. Wu, X. Zhou, J. Xu, W. Zhu, Y. Shu and P. Liu, Future Oncol 10, 1795-
803 1807 (2014) doi: 10.2217/fon.14.30
804
805 71 T.A. Thibaudeau and D.M. Smith, Pharmacol Rev 71, 170-197 (2019) doi:
806 10.1124/pr.117.015370
807
808 72 A.K. Deshantri, J.M. Metselaar, S. Zagkou, G. Storm, S.N. Mandhane, M. Fens and
809 R.M. Schiffelers, Int J Pharm X 1, 100011 (2019) doi: 10.1016/j.ijpx.2019.100011
810
811 73 S. Best, T. Hashiguchi, A. Kittai, N. Bruss, C. Paiva, C. Okada, T. Liu, A. Berger and
812 A.V. Danilov, Blood Adv 3, 51-62 (2019) doi: 10.1182/bloodadvances.2018026880
813
814 74 T. Metsalu and J. Vilo, Nucleic Acids Res 43, W566-570 (2015) doi:
815 10.1093/nar/gkv468
816
817 75 R.A. Moffitt, R. Marayati, E.L. Flate, K.E. Volmar, S.G. Loeza, K.A. Hoadley, N.U.
818 Rashid, L.A. Williams, S.C. Eaton, A.H. Chung, J.K. Smyla, J.M. Anderson, H.J. Kim, D.J.
819 Bentrem, M.S. Talamonti, C.A. Iacobuzio-Donahue, M.A. Hollingsworth and J.J. Yeh, Nat
820 Genet 47, 1168-1178 (2015) doi: 10.1038/ng.3398
821

76 M.V. Kuleshov, M.R. Jones, A.D. Rouillard, N.F. Fernandez, Q. Duan, Z. Wang, S. Koplev, S.L. Jenkins, K.M. Jagodnik, A. Lachmann, M.G. McDermott, C.D. Monteiro, G.W. Gundersen and A. Ma'ayan, Nucleic Acids Res 44, W90-97 (2016) doi: 10.1093/nar/gkw377

77 Y. Benjamini, D. Drai, G. Elmer, N. Kafkafi and I. Golani, Behav Brain Res 125, 279-284 (2001) doi: 10.1016/s0166-4328(01)00297-2

78 J. von Burstin, S. Eser, M.C. Paul, B. Seidler, M. Brandl, M. Messer, A. von Werder, A. Schmidt, J. Mages, P. Pagel, A. Schnieke, R.M. Schmid, G. Schneider and D. Saur, Gastroenterology 137, 361-371, 371 e361-365 (2009) doi: 10.1053/j.gastro.2009.04.004

79 J.M. Ossewaarde, A. de Vries, T. Bestebroer and A.F. Angulo, Appl Environ Microbiol 62, 328-331 (1996)

80 S. Diersch, M. Wirth, C. Schneeweis, S. Jors, F. Geisler, J.T. Siveke, R. Rad, R.M. Schmid, D. Saur, A.K. Rustgi, M. Reichert and G. Schneider, Oncogene 35, 3880-3886 (2016) doi: 10.1038/onc.2015.437

81 C.L. Christensen, N. Kwiatkowski, B.J. Abraham, J. Carretero, F. Al-Shahrour, T. Zhang, E. Chipumuro, G.S. Herter-Sprie, E.A. Akbay, A. Altabef, J. Zhang, T. Shimamura, M. Capelletti, J.B. Reibel, J.D. Cavanaugh, P. Gao, Y. Liu, S.R. Michaelsen, H.S. Poulsen, A.R. Aref, D.A. Barbie, J.E. Bradner, R.E. George, N.S. Gray, R.A. Young and K.K. Wong, Cancer Cell 26, 909-922 (2014) doi: 10.1016/j.ccell.2014.10.019

847 **Figure legends**

848 **Figure 1** *Drug screening in human PDAC cells with diverse MYC activity*.

849 **A)** MYC protein expression analysis of the four indicated PDAC cell lines was determined by
850 western blotting. ACTB (beta-actin) served as a loading control. **B)** GSEA by GeneTrail2 1.6
851 web service demonstrates enrichment of the depicted MYC signatures in the MYC^{high} lines.
852 Color coded enrichment score (ES) is depicted. *** adjusted p values<0.001; **** adjusted p
853 values<0.0001. **C)** Strategy for drug screening experiments with of n=129 FDA-approved
854 anticancer drugs. Cells were treated for 72h (two doubling times) with 600nM of each
855 compound. Hits were determined as a two-fold difference in responsiveness. **D)** Top ten hits
856 from the drug screening of 129 FDA-approved compounds depicted as a variance scaled
857 heatmap.

858 **Figure 2** *Validation of the drug screening experiment*.

859 **A)** Quantification of MYC expression of the indicated cell lines. In three independent lysates
860 the MYC expression was determined and shown is the mean MYC expression per cell lines.
861 *p value of an unpaired t-test <0.05. **B)** Viability for multi-dose treatment of MYC^{high} and MYC^{low}
862 cells of displayed compounds. Cells were treated for 72h and viability was measured by MTT.
863 Each dose-response experiment was conducted in three independent biological experiments
864 conducted as technical triplicates. The area under the dose response curves (AUC) in both
865 groups is depicted for each drug. **C)** Venn-diagram of data from the DoRothEA (Discriminant
866 Regulon Expression Analysis) database and our drug screening hits. Significant (FDRq <0.05)
867 drug-MYC interactions of the DoRothEA database were compared to the hits of our
868 experimental drug screening experiment. Drugs hits were summarized into drug classes.

869 **Figure 3** *Pathways enriched in human common MYC^{high} PDACs.*

870 **A)** Clustering of the ICGC PDAC mRNA expression dataset according to the genes of the
871 HALLMARK_MYC_TARGETS_V1 signature. Color coded information of the Histology, the
872 Subtype and the MYC activity state determined by clustering of the
873 HALLMARK_MYC_TARGETS_V1, the HALLMARK_MYC_TARGETS_V2 and the MUHAR
874 MYC TARGETS [31] are depicted. **B)** Venn diagram of PDAC identified as MYC^{high} by

clustering of the genes of the depicted signatures in the ICGC dataset. 8 PDACs were identified as common MYC^{high} PDACs. **C)** Common MYC^{high} PDACs of the TCGA and the ICGC dataset were analyzed by GSEA using the HALLMARK, the KEGG, the RREACTOME, and the GO-TERM signatures of the MSigDB with a FDR q value threshold of <0.25. The Venn diagram depicts 603 signatures enriched in common MYC^{high} PDACs of both datasets. **D)** NES visualized by a heatmap of the HALLMARK and the KEGG signatures enriched in common MYC^{high} PDACs of both datasets. **E)** NES visualized by a heatmap of gene signatures of the UPR and UPR-associated pathways enriched in common MYC^{high} PDACs of both datasets. As a control, IMIM-PC1^{MYCER} cells were used. Shown is the NES of the same signatures enriched in 4-OHT treated (MYC on) cells. For all depicted signatures: FDR q<0.05.

Figure 4 *MYC primes for proteasome inhibitor induced apoptosis.*

A) Bortezomib sensitivities of human PDAC cell lines from the PRISM repurposing primary screen (19Q3) [39], the GDSC2 screen (AUC) [40], and the CTD^2 (AUC) screen [41] were divided into quartiles and lines for the most sensitive quartile were compared to the remaining cell lines of the complete CCLE PDAC dataset with a gene set enrichment analysis using the GeneTrail2 1.6 web service. The enrichment score was color coded. **** adjust. p-value<0.0001. **B)** Growth inhibitory 50% concentration of n=38 murine PDAC cell lines for Bortezomib and Marizomib was determined (72h of treatment, seven-point dilution, MTT assay, non-linear regression, n=3 independent biological replicates as technical triplicates). Depicted is the Pearson correlation coefficient and the linear regression (in red). **C)** Bortezomib and Marizomib GI_{50} values were divided into quartiles and lines from the most sensitive quartile were compared to the remaining cell lines by GSEA. In addition, the lines belonging to the Bortezomib as well as the Marizomib most sensitive quartile were compared to the rest of the lines by GSEA. GSEA was conducted by the GeneTrail2 1.6 web service. Color coded enrichment score is depicted. **adj. p-value<0.01, ***adj. p-value<0.001, ****adj. p-value<0.0001. **D)** Western blot analysis to determine expression of MYC, cleaved PARP and ACTB (loading control), 8 and 24 hours after treatment with 50nM Bortezomib or DMSO (vehicle control) (n=3). E) The cleaved PARP band was quantified in three independent

expriments and the mean fold induction of cleaved PARP expression in MYC^{low} and MYC^{high} subtypes is depicted. **F)** Determination of CRISPR/Cas9 mediated knockout of the NOXA gene in MiaPaCa2 cells by PCR. A product size of 137 bp indicates the wild type allele, while no product indicates NOXA knockout a cells as described in MM section. **G)** Clonogenic growth assay of Bortezomib treated MiaPaCa-2 NOXA knockouts and wildtype cells with the indicated concentrations. One representative experiment out of three is depicted. **H)** Quantification of three independent clonogenic growth assays according to G). *p value of an unpaired t-test<0.001.

Figure 5 *Proteasome inhibitor sensitivity and MYC – genetic gain- and loss-of function.*

A) Scheme of floxed MYC alleles, which can be deleted by Cre^{ERT2} recombinase upon treatment with 4-OHT (4-Hydroxytamoxifen). E1-E3: Exon1-Exon3; 4-OHT: 4-Hydroxytamoxifen. **B)** Protein expression of MYC and beta actin (loading control) in EtOH and 4-Hydroxytamoxifen PDAC cells 72h after treatment. Displayed are 3 independent biological replicates. **C)** Quantification of MYC protein expression, determined by western blot (n=3). **D)** Relative viability of PDAC cells, 72h after treatment with Bortezomib. Cells were pretreated with EtOH and 4-Hydroxytamoxifen for 24h. Viability was measured by MTT-test. P value of an unpaired t-test is depicted (n=3). **E)** Quantitative PCR of indicated targets 72h after treatment with 600nM 4-OHT. *Gapdh* served as housekeeping control (n=3). **F)** Viability test by CellTiterGlo of PSN1 and PPT-9091-MYC^{ER} cell lines. 2.000 cells were seeded and after 24h treated with 600nM 4-OHT (MYC^{ER} shuttles into nucleus) or EtOH (vehicle) and 7 increasing concentrations of Bortezomib for three days; highest conc.: 100nM. **J)** 6 days treatment with 600nM of 4-OHT, and simultaneous treatment with Bortezomib 24h after seeding of 1.000 cells/well similar to (H). **K)** Treatment for 3d with 600nM 4-OHT and subsequent 3d treatment with Bortezomib without 4-OHT treatment according to (I). For I-K the standard deviation (SD) was used for error bars and three independent biological replicates were conducted as technical triplicates.

Supplementary Information

Table S1 *Doubling time of PDAC cell lines used for the drug screening experiment.*

Panc1, PaTu8988S, DanG and PSN1 cells were seeded in 96 well plates at a density of 3000 cells/well. After 24, 48h, 72h and 96h viable cells were measured by MTT-test to determine doubling time of the cell lines.

Table S2 *Complete list of the response to compounds used in the drug screen.*

PSN1, Panc1, PaTu8988S and DanG cells were treated with n=129 compounds in biological and technical triplicates. Drug response as well as mean of MYC high and mean of MYC low are displayed.

Table S3 *Pathways associated with MYC in common MYC^{high} PDAC.*

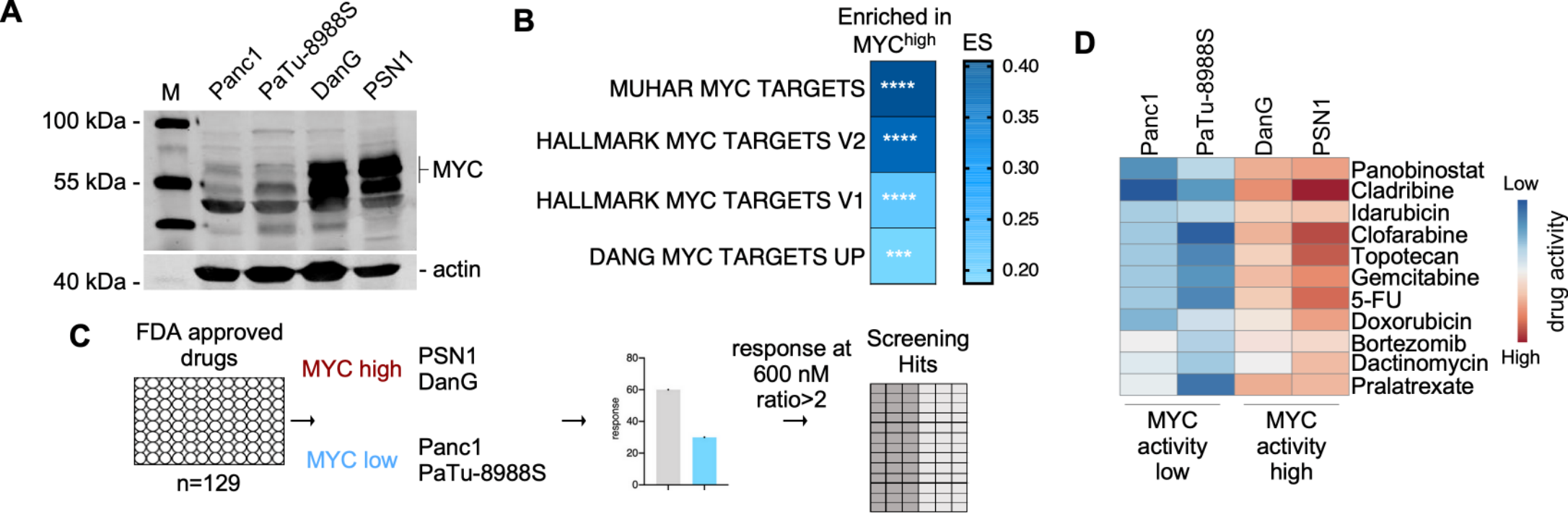
GSEA of pathways enriched in common MYC^{high} PDAC of the ICGC and the TCGA dataset.

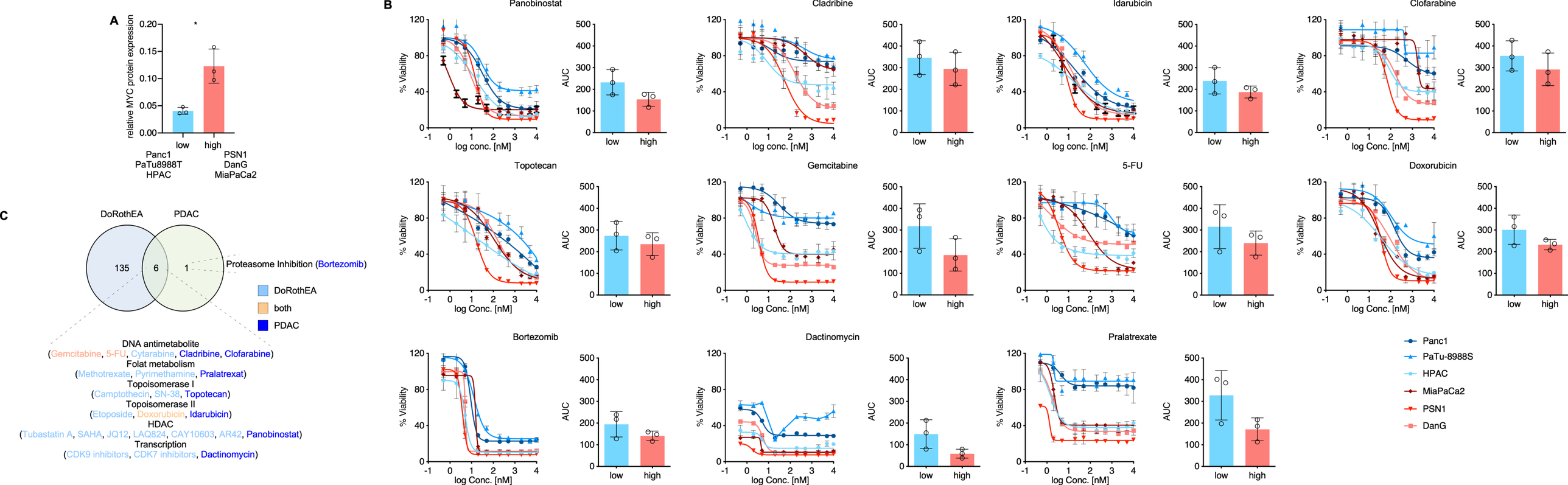
SFigure 1 *Survival and Subtypes of common MYC^{high} PDACs.*

A) Survival data of common MYC^{high} PDACs of the ICGC dataset are displayed in a Kaplan-Meyer-Curve. P value of a log-rank test is depicted. **B)** Percentage of squamous subtype of the common MYC^{high} PDACs compared to the others. Fisher Exact test: $p<0.0001$. **C)** Venn diagram of PDAC identified as MYC^{high} by clustering of the genes of the depicted signatures in the TCGA dataset. 16 PDACs were identified as common MYC^{high} PDACs. **D)** Survival data of common MYC^{high} PDACs of the TCGA dataset are displayed in a Kaplan-Meyer-Curve. **E)** Percentage of basal-like subtype of the common MYC^{high} PDACs compared to the others. Fisher Exact test: $p<0.05$. F) GSEA of IMIM-PC1^{MYCER} cells treated with 4-OHT to activate MYC. Depicted are HALLMARK and KEGG signature corresponding to the tissue-based analysis corresponding to Fig. 3D. The NES and the FDR q values are depicted.

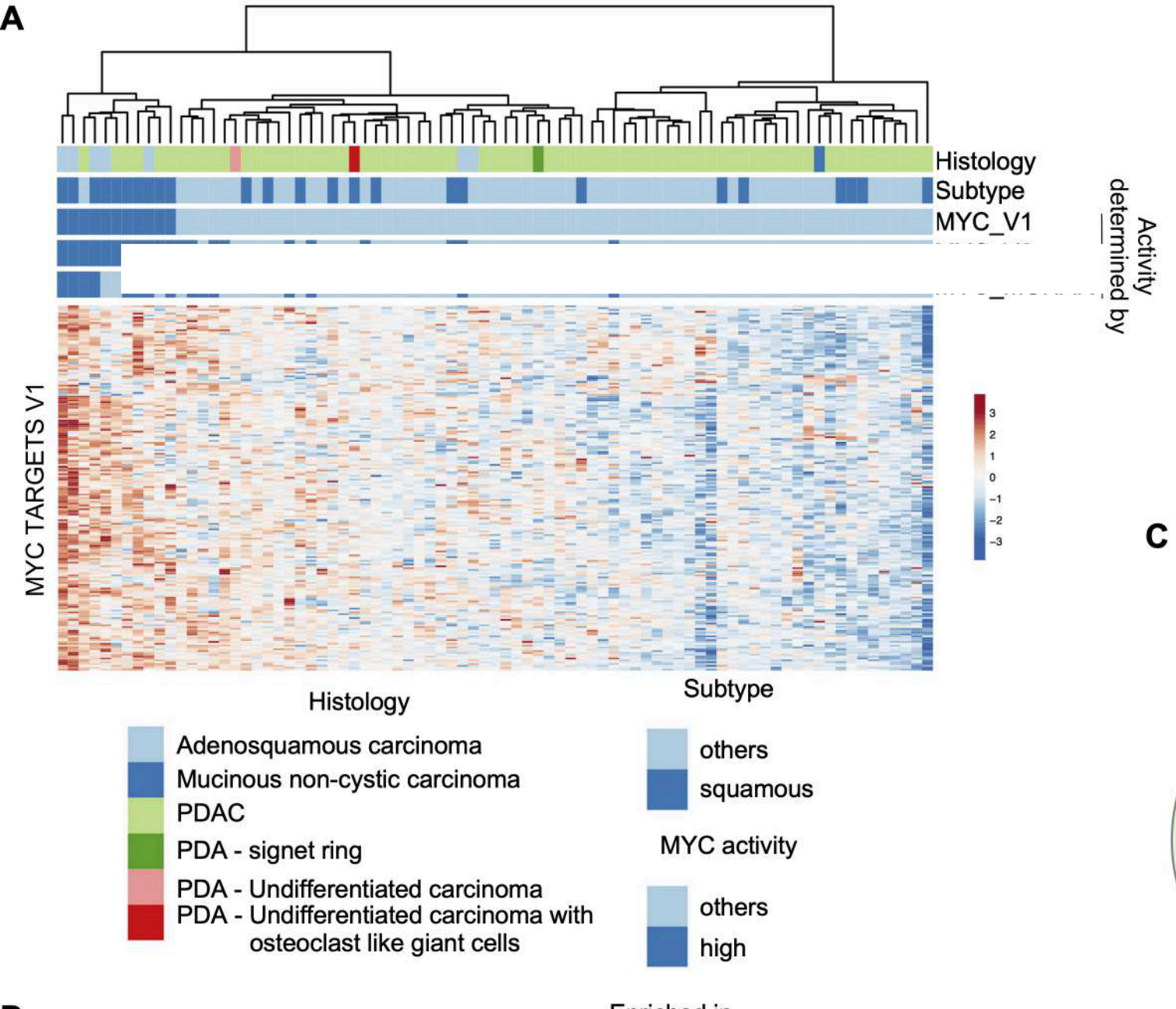
SFigure 1 *Association of MYC with perturbants of the protein homeostasis.*

Sensitivities of human PDAC cell lines from the PRISM repurposing primary screen (19Q3) [39] of the depicted drug classes were divided into quartiles and lines for the most sensitive quartile were compared to the remaining cell lines of the complete CCLE PDAC dataset with a gene set enrichment analysis using the GeneTrail2 1.6 web service. The enrichment score was color coded. ** adjust. p-value<0.01; **** adjust. p-value<0.0001.

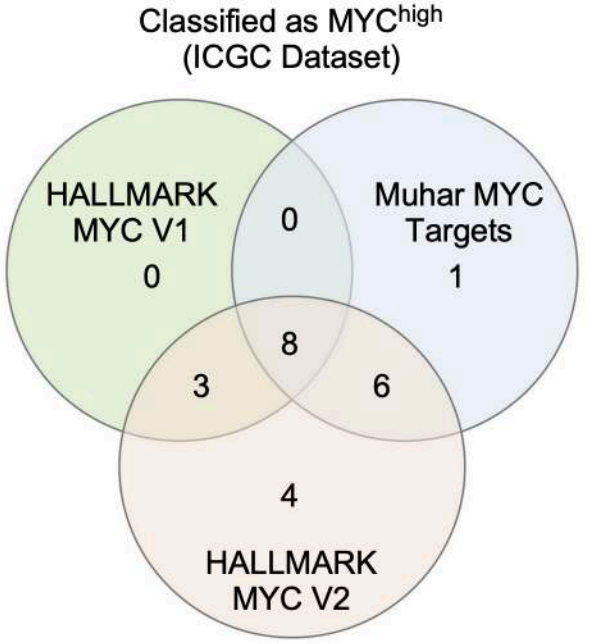

A
M
Panc1
PaTu-8988S
DanG
PSN1
100 kDa -
55 kDa -
40 kDa -
MYC
- actin
B
Enriched in MYC^high
ES
MUHAR MYC TARGETS
HALLMARK MYC TARGETS V2
HALLMARK MYC TARGETS V1
DANG MYC TARGETS UP
****
****
****
***
0.40
0.35
0.30
0.25
0.20
C
FDA approved drugs
n=129
MYC high
PSN1
DanG
MYC low
Panc1
PaTu-8988S
response
response at 600 nM ratio>2
Screening Hits
D
Panc1
PaTu-8988S
DanG
PSN1
Panobinostat
Cladribine
Idarubicin
Clofarabine
Topotecan
Gemcitabine
5-FU
Doxorubicin
Bortezomib
Dactinomycin
Pralatrexate
MYC activity low
MYC activity high
Low
High
drug activity


A
relative MYC protein expression
0.20
0.15
0.10
0.05
0.00
*
low
high
Panc1
PaTu8988T
HPAC
PSN1
DanG
MiaPaCa2
B
Panobinostat
Cladribine
Idarubicin
Clofarabine
Topotecan
Gemcitabine
5-FU
Doxorubicin
Bortezomib
Dactinomycin
Pralatrexate
% Viability
AUC
log conc. [nM]
log Conc. [nM]
Panc1
PaTu-8988S
HPAC
MiaPaCa2
PSN1
DanG
C
DoRothEA
PDAC
135
6
1
Proteasome Inhibition (Bortezomib)
DoRothEA
both
PDAC
DNA antimetabolite
(Gemcitabine, 5-FU, Cytarabine, Cladribine, Clofarabine)
Folat metabolism
(Methotrexate, Pyrimethamine, Pralatrexat)
Topoisomerase I
(Camptothecin, SN-38, Topotecan)
Topoisomerase II
(Etoposide, Doxorubicin, Idarubicin)
HDAC
(Tubastatin A, SAHA, JQ12, LAQ824, CAY10603, AR42, Panobinostat)
Transcription
(CDK9 inhibitors, CDK7 inhibitors, Dactinomycin)

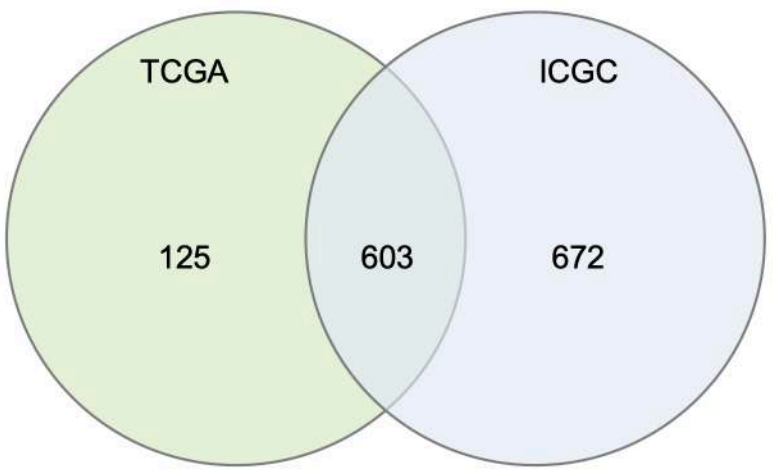
A


Histology
Subtype
MYC_V1
Activity determined by
MYC TARGETS V1
3
2
1
0
−1
−2
−3
Histology
Subtype
Adenosquamous carcinoma
Mucinous non-cystic carcinoma
PDAC
PDA - signet ring
PDA - Undifferentiated carcinoma
PDA - Undifferentiated carcinoma with osteoclast like giant cells
others
squamous
MYC activity
others
high

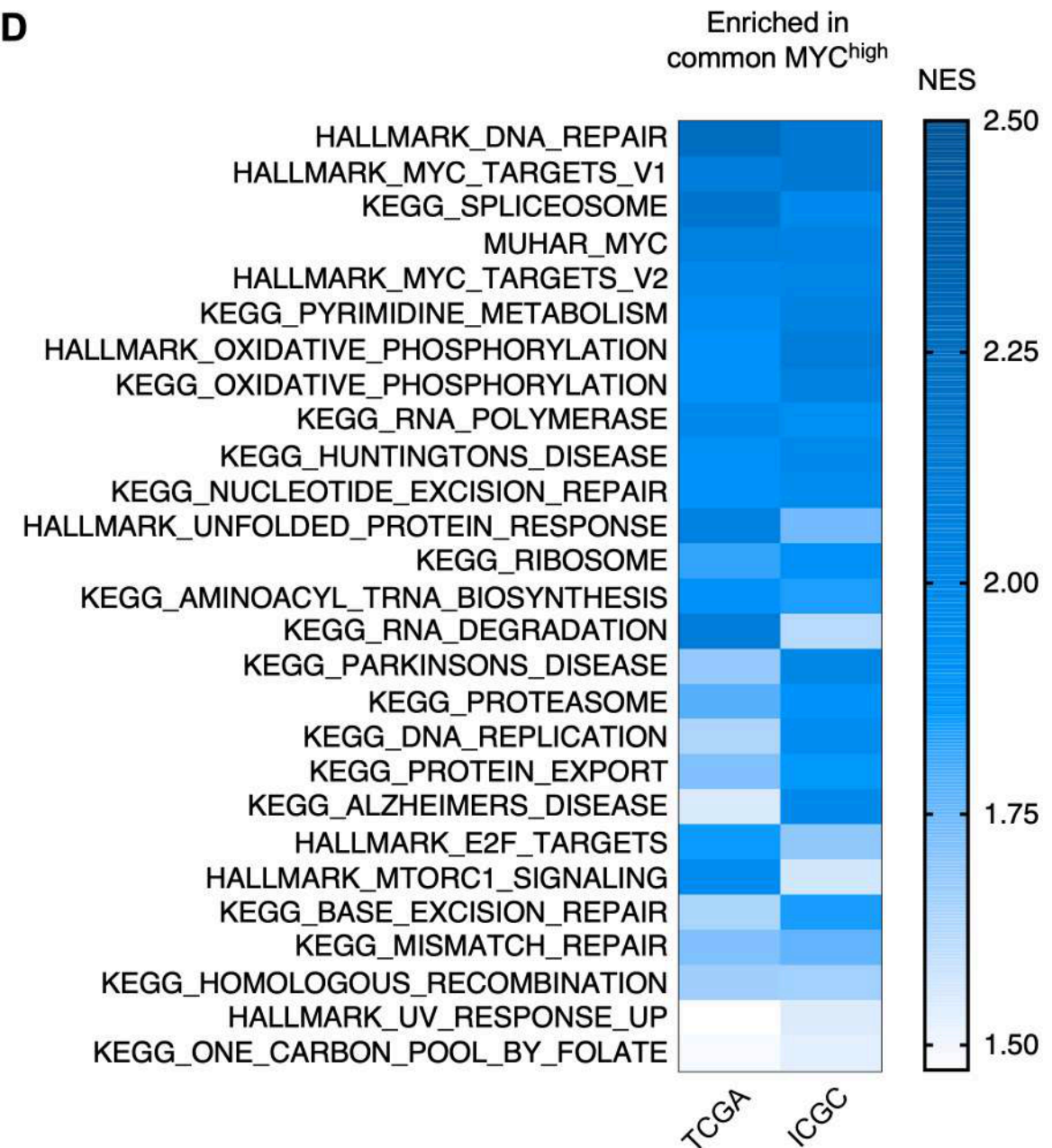
B


Classified as MYC^high
(ICGC Dataset)
HALLMARK MYC V1
0
Muhar MYC Targets
1
0
8
3
6
4
HALLMARK MYC V2

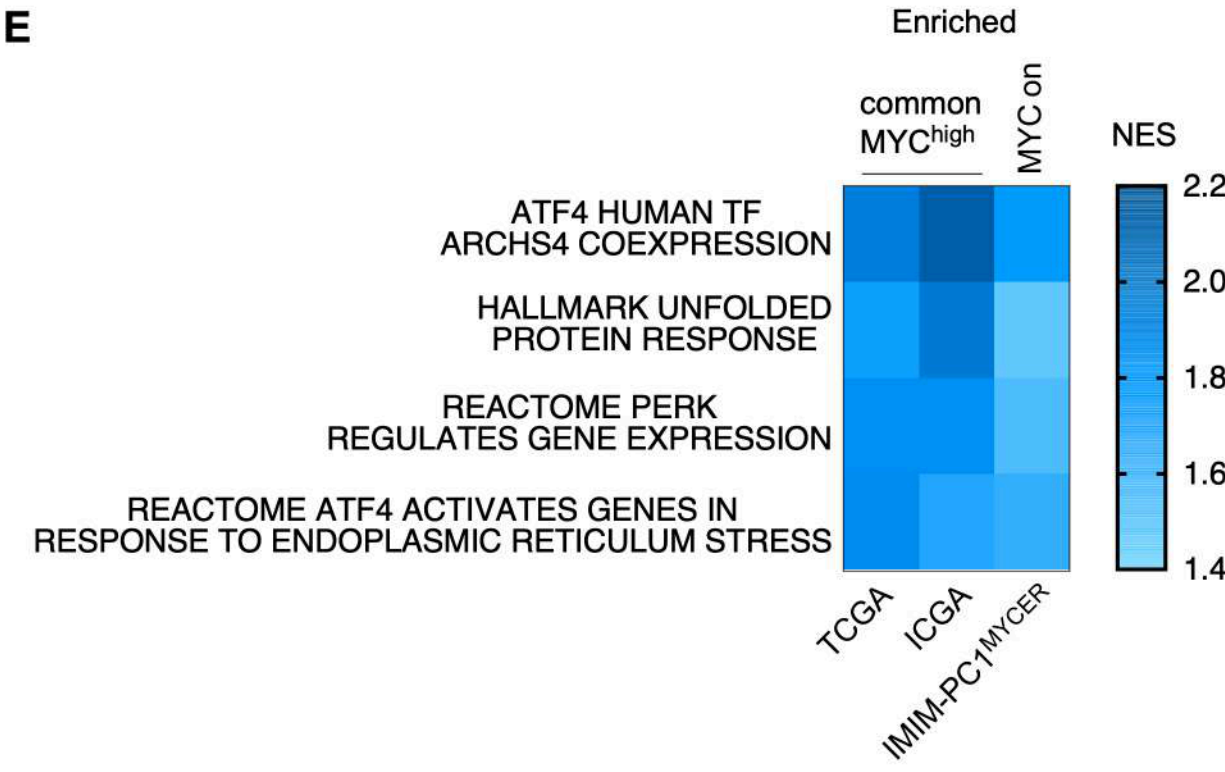
C

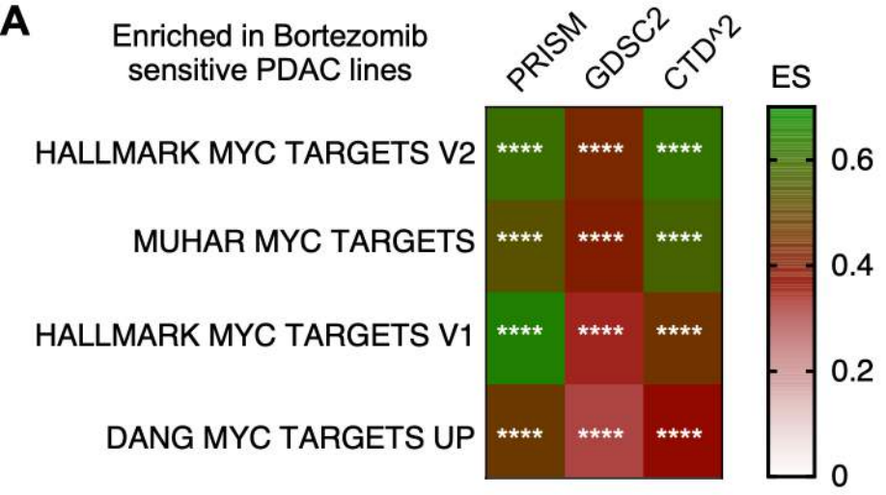

Signatures enriched in common MYC^high
(HALLMARK, KEGG, GO-Term, REACTOME)
TCGA
ICGC
125
603
672

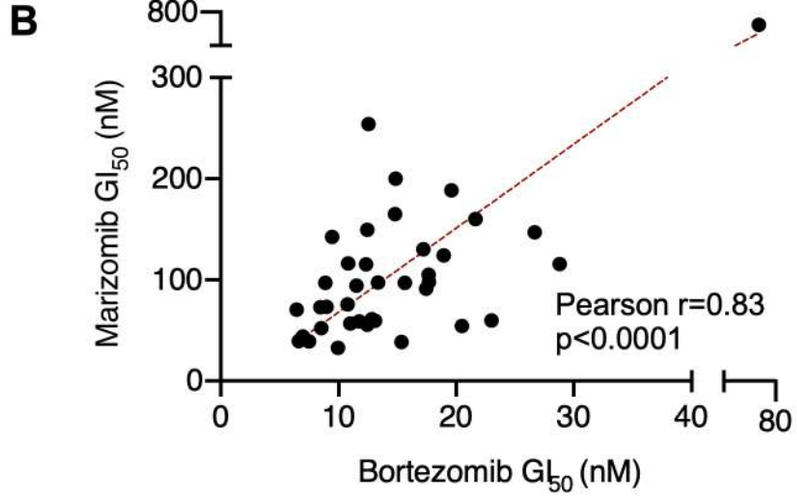
D

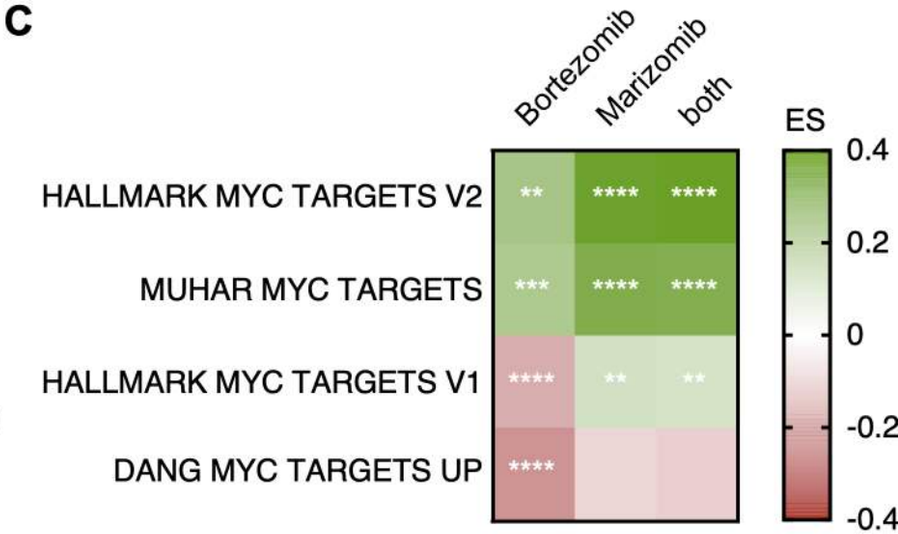

Enriched in common MYC^high
NES
HALLMARK_DNA_REPAIR
HALLMARK_MYC_TARGETS_V1
KEGG_SPLICEOSOME
MUHAR_MYC
HALLMARK_MYC_TARGETS_V2
KEGG_PYRIMIDINE_METABOLISM
HALLMARK_OXIDATIVE_PHOSPHORYLATION
KEGG_OXIDATIVE_PHOSPHORYLATION
KEGG_RNA_POLYMERASE
KEGG_HUNTINGTONS_DISEASE
KEGG_NUCLEOTIDE_EXCISION_REPAIR
HALLMARK_UNFOLDED_PROTEIN_RESPONSE
KEGG_RIBOSOME
KEGG_AMINOACYL_TRNA_BIOSYNTHESIS
KEGG_RNA_DEGRADATION
KEGG_PARKINSONS_DISEASE
KEGG_PROTEASOME
KEGG_DNA_REPLICATION
KEGG_PROTEIN_EXPORT
KEGG_ALZHEIMERS_DISEASE
HALLMARK_E2F_TARGETS
HALLMARK_MTORC1_SIGNALING
KEGG_BASE_EXCISION_REPAIR
KEGG_MISMATCH_REPAIR
KEGG_HOMOLOGOUS_RECOMBINATION
HALLMARK_UV_RESPONSE_UP
KEGG_ONE_CARBON_POOL_BY_FOLATE
2.50
2.25
2.00
1.75
1.50
TCGA
ICGC

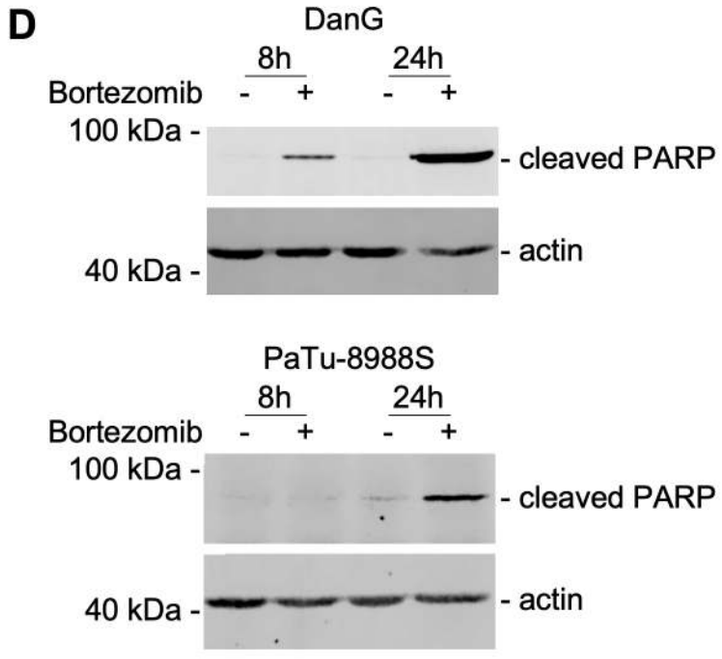
E

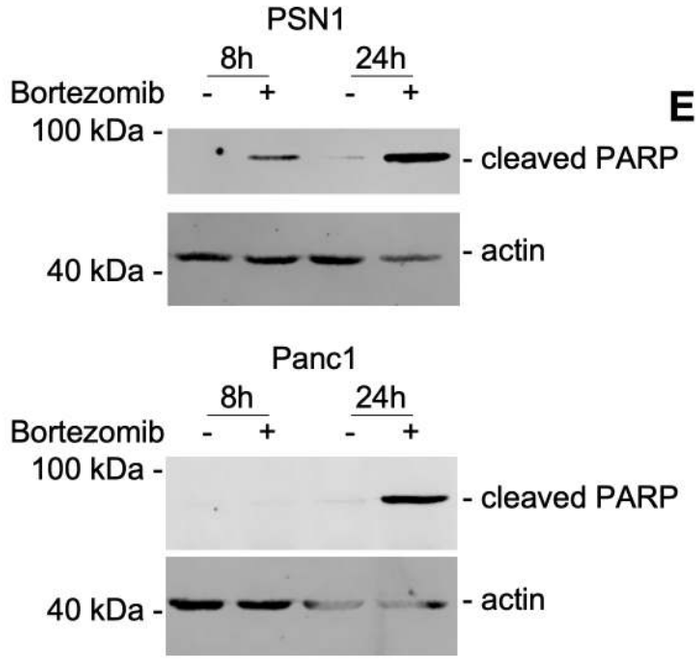

Enriched
common MYC^high
MYC on
NES
ATF4 HUMAN TF ARCHS4 COEXPRESSION
HALLMARK UNFOLDED PROTEIN RESPONSE
REACTOME PERK REGULATES GENE EXPRESSION
REACTOME ATF4 ACTIVATES GENES IN RESPONSE TO ENDOPLASMIC RETICULUM STRESS
2.2
2.0
1.8
1.6
1.4
TCGA
ICGA
IMIM-PC1^MYCER

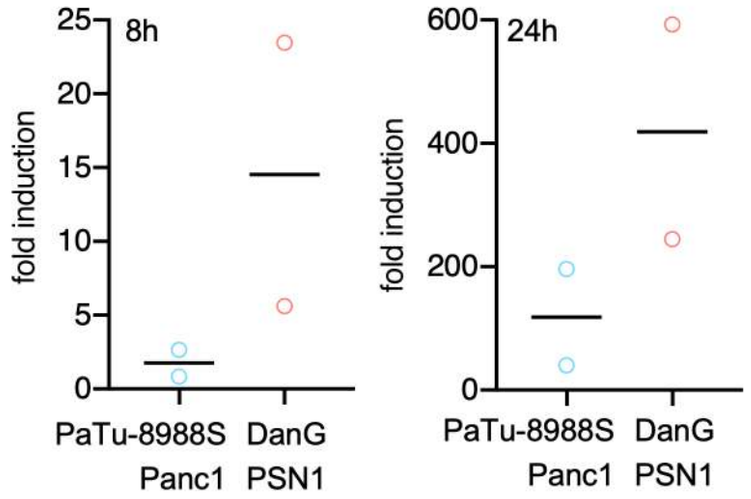

A
Enriched in Bortezomib sensitive PDAC lines
PRISM
GDSC2
CTD^2
ES
HALLMARK MYC TARGETS V2
MUHAR MYC TARGETS
HALLMARK MYC TARGETS V1
DANG MYC TARGETS UP
0.6
0.4
0.2
0

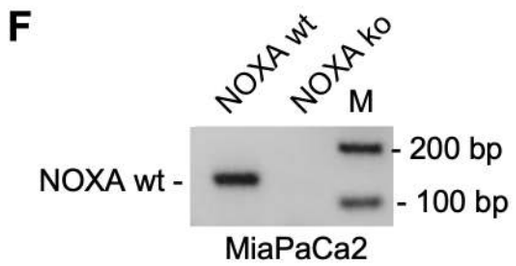

B
Marizomib GI50 (nM)
Bortezomib GI50 (nM)
Pearson r=0.83
p<0.0001

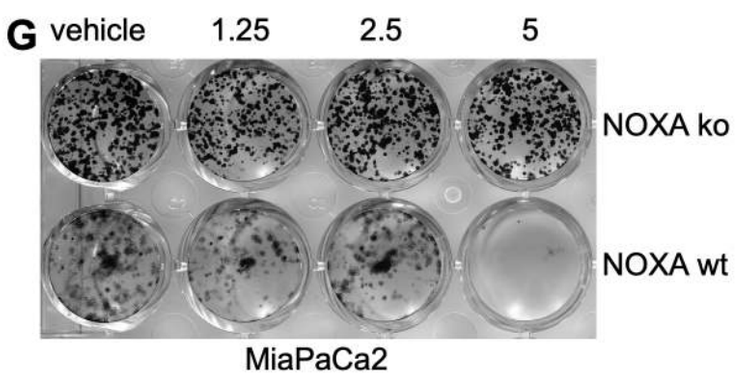

C
Bortezomib
Marizomib
both
ES
HALLMARK MYC TARGETS V2
MUHAR MYC TARGETS
HALLMARK MYC TARGETS V1
DANG MYC TARGETS UP
0.4
0.2
0
-0.2
-0.4

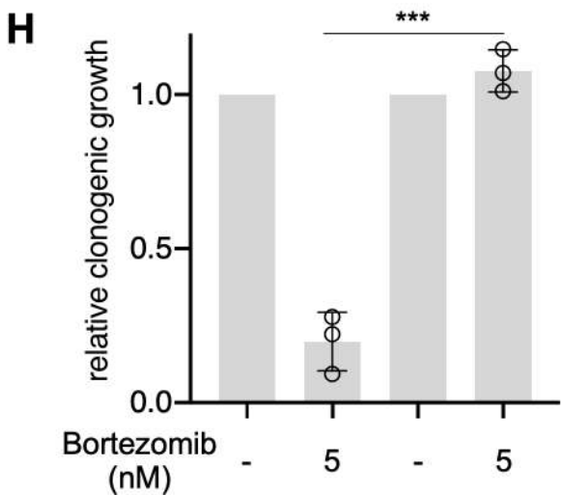

D
DanG
8h
24h
Bortezomib
100 kDa -
- cleaved PARP
40 kDa -
- actin
PaTu-8988S

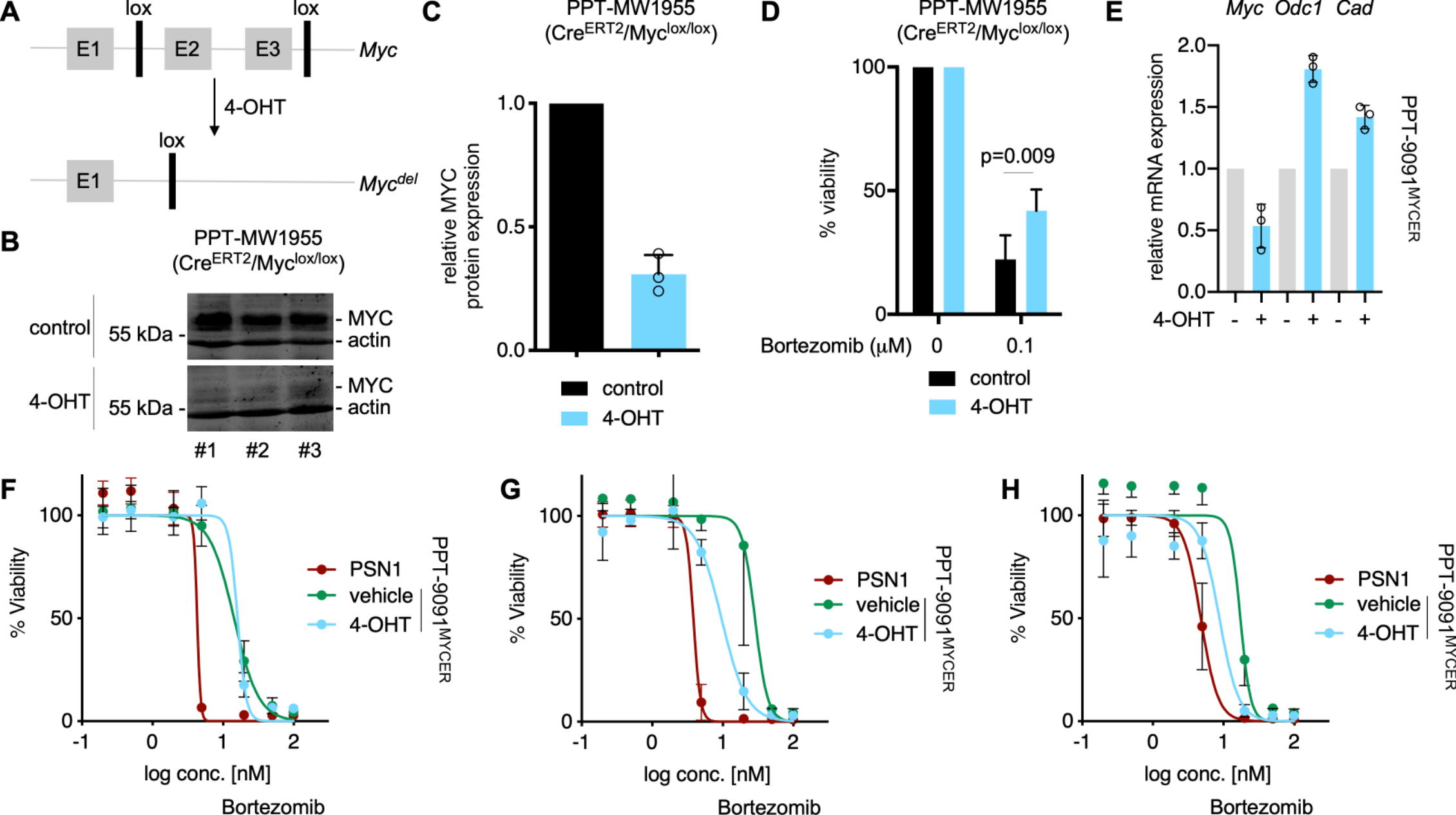

PSN1
8h
24h
Bortezomib
100 kDa -
- cleaved PARP
40 kDa -
- actin
Panc1


E
8h
24h
fold induction
PaTu-8988S
DanG
Panc1
PSN1


F
NOXA wt
NOXA ko
M
NOXA wt -
- 200 bp
- 100 bp
MiaPaCa2


G
vehicle
1.25
2.5
5
NOXA ko
NOXA wt
MiaPaCa2


H
***
relative clonogenic growth
Bortezomib (nM)


A
lox
lox
E1
E2
E3
Myc
4-OHT
lox
E1
Myc^del
B
PPT-MW1955
(Cre^ERT2/Myc^lox/lox)
control
55 kDa -
- MYC
- actin
4-OHT
55 kDa -
- MYC
- actin
#1
#2
#3
C
PPT-MW1955
(Cre^ERT2/Myc^lox/lox)
relative MYC
protein expression
1.0
0.5
0.0
control
4-OHT
D
PPT-MW1955
(Cre^ERT2/Myc^lox/lox)
% viability
100
50
0
p=0.009
Bortezomib (μM)
0
0.1
control
4-OHT
E
Myc
Odc1
Cad
relative mRNA expression
2.0
1.5
1.0
0.5
0.0
4-OHT
-
+
-
+
-
+
PPT-9091^MYCER
F
% Viability
100
50
0
-1
0
1
2
log conc. [nM]
Bortezomib
PSN1
vehicle
4-OHT
PPT-9091^MYCER
G
% Viability
100
50
0
-1
0
1
2
log conc. [nM]
Bortezomib
PSN1
vehicle
4-OHT
PPT-9091^MYCER
H
% Viability
100
50
0
-1
0
1
2
log conc. [nM]
Bortezomib
PSN1
vehicle
4-OHT
PPT-9091^MYCER